1   Dated 05 Sep 2024 – submitted to Ocean Science

2   **TEOS-10 and the Climatic Relevance of Ocean-Atmosphere Interaction**

3   Rainer Feistel

4   Leibniz Institute for Baltic Sea Research (IOW), 18119 Warnemünde, Germany

5   **Correspondence**: Rainer Feistel (rainer.feistel@io-warnemuende.de)

6   **Abstract**: Unpredicted observations in the climate system, such as recently an excessive ocean
7   warming, are often lacking immediate causal explanations and are challenging the numerical models.
8   As a highly advanced mathematical tool, the Thermodynamic Equation of Seawater – 2010 (TEOS-10)
9   had been established by international bodies as an interdisciplinary standard and is recommended
10   for use in geophysics, such as especially in climate research. From its very beginning, the
11   development of TEOS-10 was supported by *Ocean Science* through publishing successive stages and
12   results. Here, the history and properties of TEOS-10 are briefly reviewed. With focus on the air-sea
13   interface, selected current problems of climate research are discussed and tutorial examples for the
14   possible use of TEOS-10 in the associated context are presented, such as related to ocean heat
15   content, latent heat and rate of marine evaporation, properties of sea spray aerosol, or climatic
16   effects of low-level clouds. Appended to this article, a list of publications and their metrics is
17   provided for illustrating the uptake of TEOS-10 by the scientific community, along with some
18   continued activities, addressing still pending, connected issues such as uniform standard definitions
19   of uncertainties, of relative humidity, seawater salinity or pH.

20   This article is dedicated to the Jubilee celebrating 20 years of Ocean Science.

21   This article is also dedicated to the memory of Wolfgang Wagner who sadly and unexpectedly has
22   passed away on 12 August 2024. His contributions to TEOS-10 are truly indispensable constituents;
23   Wolfgang was an essential co-author of various related documents and articles. He will deeply be
24   missed.

26   *All the rivers run into the sea; yet the sea is not full;*
27   *unto the place from whence the rivers come, thither they return again.*
28   The King James Bible: Ecclesiastes, 450 – 150 BCE

29   *He wraps up the waters in his clouds,*
30   *yet the clouds do not burst under their weight.*
31   Holy Bible: New International Version, Job 26:8

32   *Of the air, the part receiving heat is rising higher.*
33   *So, evaporated water is lifted above the lower air.*
34   Leonardo da Vinci: Primo libro delle acque, Arundel Codex, ca. 1508

35   *Two-thirds of the Sun's energy falling on the Earth's surface is needed*
36   *to vaporize ... water ... as a heat source for a gigantic steam engine.*
37   Heinrich Hertz: Energiehaushalt der Erde, 1885

38   *The sea surface interaction is obviously*
39   *a highly significant quantity in simulating climate.*
40   Andrew Gilchrist, Klaus Hasselmann: Climate Modelling, 1986

The climate of the Earth is ultimately determined
by the temperatures of the oceans.
Donald Rapp: Assessing Climate Change, 2014

1 Introduction

Quite recently in 2024, climate research has published alarming news: "The world's oceans absorbed more heat in 2023 than in any other year since records began in the 1950s. … Data show that the heat stored in the upper 2,000 metres of oceans increased by 15 zettajoules (1 zettajoule is 10^{21} joules) in 2023 compared with that stored in 2022. This is an enormous amount of energy — for comparison, the world's total energy consumption in 2022 was roughly 0.6 zettajoules" (You 2024: p. 434). Dividing this value by the global ocean surface area and by the duration of a year, the reported ocean's average warming rate amounts to 1.3 W m^{-2}, and is apparently even increasing. "Earth's net global energy imbalance (12 months up to September 2023) amounts to +1.9 W m^{-2}, … ensuring further heating of the ocean" (Kuhlbrodt et al. 2024: p. E474). „Climate models struggle to explain why planetary temperatures spiked suddenly. … No year has confounded climate scientists' predictive capabilities more than 2023. … This sudden heat spike greatly exceeds predictions made by statistical climate models" (Schmidt 2024: p. 467).

The currently observed *ocean heat content* (OHC) represents a merely transient maximum after a decade-long systematic warming process in the past, see Fig. 18 in **Section 6**, which may proceed to even higher values in the future. In **Section 3**, thermodynamic aspects of related OHC definitions will be considered. Regarding the long-term period since 1971, "the drivers of a larger Earth energy imbalance in the 2000s than [before] are still unclear. … Future studies are needed to further explain the drivers of this change" (von Schuckmann et al. 2023: p. 1694). Laterally, the observed heat excess is unevenly distributed over the world ocean (Fig. 1), in contrast to what naively may be expected from rising atmospheric CO_2 concentrations. Rather, warming seems to be most pronounced in the cloudy austral and boreal west-wind belts. Selected thermodynamic relations between OHC and cloudiness are briefly discussed in **Section 6**.
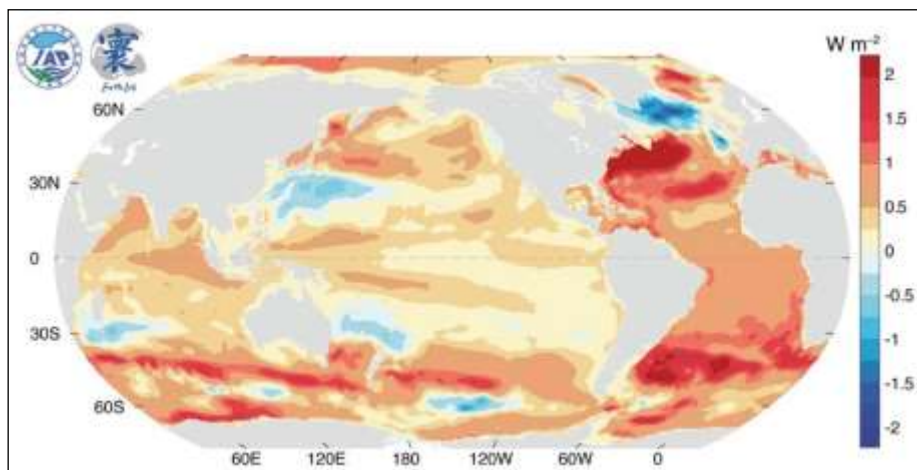
Fig. 1: Observed trend 1958 through 2022 of the upper 2000 m ocean heat content (WMO 2024). Image reproduction permitted by WMO Copyright.

Sunlight is the only available heat source of sufficient power to cause the observed warming, while the globally averaged geothermal heat flux is estimated to be just 0.087 W m^{-2} (Pollack et al. 1993),

74 and is not expected to suddenly rise recently due to human impact. Irradiation is hampered by
75 clouds, dust and absorbing gases, and water surface reflection such as by whitecaps, waves or
76 plankton layers (Cahill et al. 2023). Heat absorbed in the water column may effectively exit the ocean
77 again only across the air-sea interface via sensible, radiative and latent heat flux. All these effects
78 may vary in the climate system in a complicated, mutually interacting manner. Typically, present
79 numerical climate models suffer from an "ocean heat budget closure problem" (Josey et al. 1999)
80 and describe the ocean-atmosphere heat flux only to within uncertainties between 10 W m^{-2} and 30
81 W m^{-2} (Josey et al. 2013). According to recent model comparison studies, many of those "models fail
82 to provide as much heat into the ocean as observed" (Weller et al. 2022: p. E1968). Dynamical
83 models, rather than observed correlations, are the most reliable tools for the detection and
84 verification of causal relations (Feistel 2023), however, such as in this case of air-sea interaction,
85 large uncertainties may prevent any significant conclusions to be drawn regarding the causes of the
86 observed ocean warming rate of 1.3 W m^{-2}.

87 Of the increasing amount of water vapour contained in the global troposphere, 85 % results from
88 ocean evaporation (Gimeno et al. 2013). Corresponding to 1200 mm annual evaporation (Budyko
89 1963, 1984, Baumgartner and Reichel 1975, Peters-Lidard et al. 2019), the associated latent heat flux
90 of about 95 W m^{-2} per ocean surface area represents the strongest energy supply for the
91 atmospheric dynamics (Albrecht 1940) and at the same time the strongest cooling process of the sea.
92 This flux depends sensitively on the relative humidity (RH) at the water surface; an RH increase by 1
93 %rh can be estimated to reduce evaporation by 5 W m^{-2} (Feistel 2015, 2024, Feistel and Hellmuth
94 2021, 2023), so that minor additional 0.2 %rh may already suffice to warm up the ocean by the
95 observed 1.3 W m^{-2}. Unfortunately, marine RH is observed only with uncertainties between 1 and 5
96 %rh (Lovell-Smith et al. 2016), or, accordingly, between 5 and 25 W m^{-2} of latent heat flux, which is
97 roughly corresponding to unknown variations ranging up to 50 … 250 mm evaporation per year. It
98 remains unclear to what extent minor, yet unnoticed changes in marine RH may be responsible for
99 the recent ocean warming.
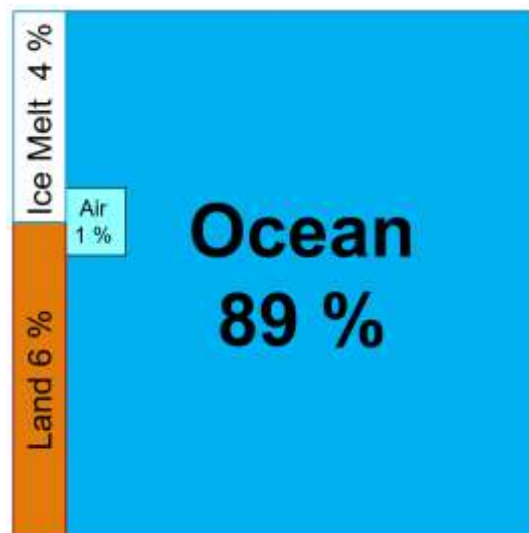
100

101 Fig. 2: Heat fractions stored additionally in the different parts of the Earth system 1960–2020 (values
102 from von Schuckmann et al. 2023), represented graphically by partial areas. Obviously, the oceans
103 dominate global warming.

104

105 According to Fig. 2, a paramount share of 94 % of global warming occurs in different phases and
106 geophysical mixtures of water, in particular in seawater. Considering this situation, the *Scientific*
107 *Committee on Oceanic Research* (SCOR) in cooperation with the *International Association for the*

108 *Physical Sciences of the Oceans* (IAPSO) decided at its 2005 Cairns meeting the establishment of the
109 *SCOR/IAPSO Working Group 127 on Thermodynamics of Seawater* (WG127) (Millero 2010, Pawlowicz
110 et al. 2012, Smythe-Wright et al. 2019), which held its inaugural meeting in 2006 at Warnemünde
111 (Fig. 3). It had been recognised that "modelling of the global heat engine needs accurate expressions
112 for the entropy, enthalpy, and internal energy of seawater so that heat fluxes can be more accurately
113 determined in the ocean" (Millero 2010: p. 28) while such properties were not available from the
114 thermodynamic seawater standard at that time, the 1980 Equation of State of Seawater (EOS-80)
115 (Fofonoff and Millard Jr. 1983).

116

117 Fig. 3: Participants of the 2006 kick-off meeting of SCOR/IAPSO WG127 at the Leibniz Institute for
118 Baltic Sea Research (IOW) in Warnemünde, Germany. From left to right: Chen-Tung Arthur Chen
119 (Taiwan), Frank Millero (USA), Brian King (UK), Rainer Feistel (WG vice chair, Germany), Daniel Wright
120 (Canada, deceased 2010), Trevor McDougall (WG chair, Australia) and Giles Marion (USA).

121

122 Fig. 4: Participants of the BIPM-IAPWS meeting in February 2012 at the Pavillon de Breteuil, Sèvres.
123 From left to right: Dan Friend (IAPWS), Karol Daučik (IAPWS president), Jeff Cooper (IAPWS), Alain
124 Picard (BIPM, deceased 2015), Petra Spitzer (WG127), Rainer Feistel (WG127), Michael Kühne
125 (director BIPM), Andy Henson (BIPM) and Robert Wielgosz (BIPM).

126

127 The foundation of WG127 happened almost coincidently with the establishment of the *Ocean*
128 *Science* journal of the *European Geosciences Union* (EGU) in 2004/05. The development of the new
129 standard by WG127, the Thermodynamic Equation of Seawater – 2010 (TEOS-10) was very
130 successfully supported by Ocean Science, publishing the Special Issue #14 on "Thermophysical
131 Properties of Seawater" with 16 articles between 2008 and 2012 (Feistel et al. 2008a). **Appendix A**

132   reports the current metrics of this Special Issue. Also in 2008, at its conference in Berlin, Germany,
133   the *International Association for the Properties of Water and Steam* (IAPWS) established a new
134   *Subcommittee on Seawater* (SCSW) that cooperated closely with WG127. In the form of carefully
135   verified mathematical formulations for properties of water, ice, seawater and humid air, IAPWS
136   adopted nine fundamental documents related to TEOS-10 (IAPWS AN6-16 2016), see **Appendix A**.

137   With respect to problems yet pending after the official adoption of TEOS-10, especially for the
138   preparation of future novel international definitions of seawater salinity, seawater pH and
139   atmospheric relative humidity (Feistel et al. 2016, Pawlowicz et al. 2016, Dickson et al. 2016, Lovell-
140   Smith et al. 2016), the standing *IAPSO/SCOR/IAPWS Joint Committee on the Properties of Seawater*
141   (JCS) was established in 2012. In 2011, IAPWS also extended its cooperation with the *International*
142   *Bureau for Weights and Measures* (BIPM), see Fig. 4. Further details on TEOS-10 (IOC et al. 2010,
143   McDougall et al. 2013, Feistel 2018, Wikipedia 2024) are available from the TEOS-10 homepage,
144   www.teos-10.org, and are briefly reviewed in **Section 2** and **Appendix B**.

145   In the context of the predecessor EOS-80, the *ocean heat content* (OHC) was defined in terms of
146   *potential temperature* (Abraham et al. 2013). Improving this method, TEOS-10 entropy and enthalpy
147   of seawater provided a proper quantitative basis for a novel, thermodynamically rigorous definition
148   of the OHC in the form of seawater *potential enthalpy* (McDougall 2003, McDougall et al. 2013,
149   Graham and McDougall 2013, McDougall et al. 2021), equivalently defined as *Conservative*
150   *Temperature* and briefly discussed in **Section 3**.
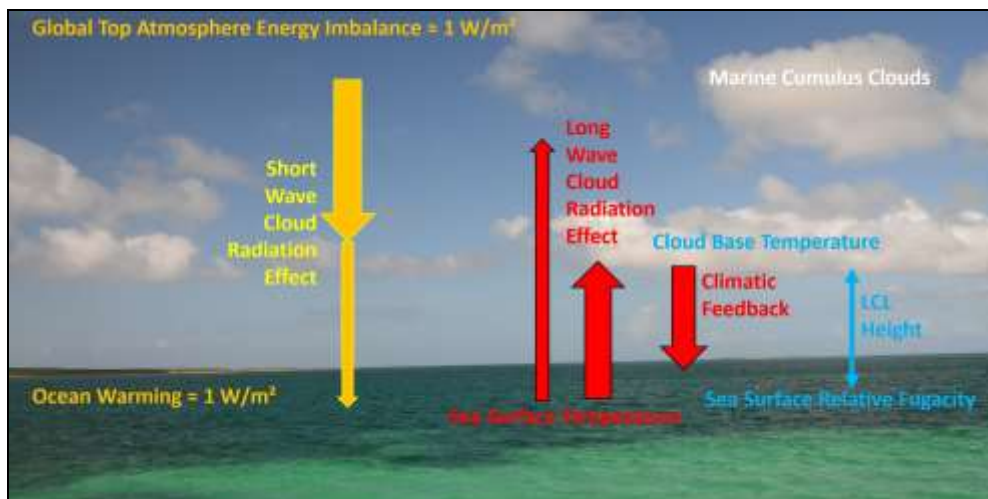
151

152   Fig. 5: Schematic of *cloud radiation effects* (CRE). The *short-wave effect* (SW CRE) controls the
153   downward flux of solar irradiation while the *long-wave effect* governs the infrared radiation balance
154   between water surface and cloud base. By thermal convection, cumulus clouds emerge at the
155   isentropic *lifted condensation level* (LCL). Figure from Feistel and Hellmuth (2024b)

156

157   Currently implemented parameterisations of marine evaporation rates in the form of historical
158   *Dalton equations* (Stewart 2008, Josey et al. 1999, 2013) may be replaced by TEOS-10 chemical
159   potentials which provide the proper quantitative basis for a thermodynamically rigorous formulation
160   of non-equilibrium Onsager forces and fluxes in terms of *relative fugacity* (RF) of humid air (Kraus
161   and Businger 1994, Feistel and Lovell-Smith 2017, Feistel and Hellmuth 2023, 2024a), as described in
162   **Section 4**. *Relative humidity* (RH) is defined relative to the saturation state of moist air, which in turn
163   is controlled by the chemical potentials of water in the gas and liquid phase. It is only natural,
164   therefore, to define RH in terms of chemical potentials, which in fact is performed by RF. The
165   uncertainty of latent heat flux with respect to the uncertainty of surface RH observation is shown to

166 be significantly larger than the observed warming of 1.3 W m^{-2}, so that this unpredicted warming
167 may or may not be caused by so-far ignored minor RH increase.

168 The conceptual model of sea air as a two-phase composite thermodynamic system is outlined in
169 **Section 5**. The roles of enthalpy, chemical potential and entropy are explained by means of explicit
170 theoretical descriptions of three simplified tutorial examples, (i) for the latent heat of evaporation,
171 (ii) for the heat capacity of humid air containing sea spray, and (iii) for the entropy production of
172 irreversible evaporation.

173 Clouds do not only release the latent heat which water vapour has carried away from the ocean, they
174 also interfere substantially in the global radiation balance, cooling the surface by reflecting short-
175 wave solar irradiation, and warming the surface by sending back down long-wave thermal radiation,
176 see Fig. 5. In the course of global warming, cloudiness has been found to exhibit a systematic trend of
177 reduction, see **Section 6**, which affects the ocean heat content in a non-trivial, non-uniform manner.
178 Marine cumulus clouds arise by isentropic uplift of thermal convection. Their height controls their
179 temperature and their thermal downward radiation, affecting the ocean's energy balance. Updating
180 previous results (Romps 2017) for the *lifted condensation level* (LCL) of marine cumulus clouds to
181 thermodynamically rigorous TEOS-10 standard equations (Feistel and Hellmuth 2024b), the radiative
182 effect of those clouds can be estimated from *sea-surface temperature* (SST) and surface relative
183 humidity. This effect turns out to be weakly cooling and cannot provide a reasonable explanation for
184 the so-far unclear strong ocean warming. The effect of increasing SST in the past decades turns out
185 to be minor in comparison to that caused by RH uncertainty.

186 **Section 7** provides a summery of this paper, **Appendix A** reports collections of publications with
187 respect to TEOS-10 as well as their metrics, and **Appendix B** gives a short introduction into the
188 concept of thermodynamic potentials.

189

190 **2 Thermodynamic Equation of Seawater – 2010 (TEOS-10)**

191 In the climate system, the omnipresent and dominant substance is water in various phases and
192 mixtures. For example, "water vapor is by far the most important greenhouse gas, in the sense that it
193 absorbs more irradiance from the Earth than all other greenhouse gases combined" (Rapp 2014: p.
194 381). Textbooks and other publications offer numerous collections of various different property
195 equations for water, ice, seawater or moist air, but uncertainties and mutual consistencies of those
196 equations are often unclear. To improve this situation, a novel *Thermodynamic Equation of Seawater*
197 *– 2010* (TEOS-10) was developed by the members of the SCOR/IAPSO Working Group 127 (WG 127)
198 in close cooperation with the International Association for the Properties of Water and Steam
199 (IAPWS). TEOS-10 is described in a detailed Manual (IOC et al. 2010) and has been adopted and
200 recommended by IOC-UNESCO (2009) in Paris and by the IUGG (2011) in Melbourne, see also Feistel
201 (2008b, 2012, 2018), Valladares et al. (2011) and Pawlowicz et al. (2012). Starting in 2008 with a
202 Special Issue of *Ocean Science* (Feistel et al. 2008a), a large number of scientific publications has
203 appeared in the meantime, supporting, extending or exploiting TEOS-10. A collection of selected
204 papers related to TEOS-10 is summarised in Appendix A together with metrics that illustrate the
205 growing uptake of TEOS-10 by the scientific community.

206 The development of the first numerical thermodynamic Gibbs potentials (see Appendix B) for
207 seawater (Feistel 1991, 1993, Feistel and Hagen 1995) was based on the works of Millero and Leung
208 (1976) and Millero (1982, 1983), together with high-pressure background data of the previous EOS-
209 80 standard (Unesco 1981). Independently of that, a Helmholtz potential for pure fluid water had
210 been adopted by IAPWS in 1996 at Fredericia (Harvey 1998, Wagner and Pruß 2002). These were the

211   key activities which eventually culminated in the formulation of TEOS-10 about two decades later. By
212   combining those equations for pure and seawater, some known pending problems of EOS-80
213   (Fofonoff and Millard Jr. 1983) could incidentally be resolved (Feistel 2003). In the end, TEOS-10 has
214   been assembled from four basic thermodynamic potentials derived from mutually consistent, most
215   comprehensive and accurate datasets of measured properties available at that time. Those
216   potentials are (IAPWS R6-95 2016, IAPWS R10-06 2009, IAPWS R13-08 2008, IAPWS G8-10 2010,
217   respectively):

218   (i)   A Helmholtz function of fluid water, $f^F(T, \rho) \equiv f^W(T, \rho) \equiv f^V(T, \rho)$, known as the
219   IAPWS-95 formulation (Wagner and Pruß 2002), which is identical for liquid water,
220          $f^W(T, \rho)$ and for water vapour, $f^V(T, \rho)$. It describes de-aerated water of a fixed
221   isotopic composition, termed *Standard Mean Ocean Water* (SMOW), with density ρ and
222   temperature T.

224   (ii)   A Gibbs function of ambient hexagonal ice I, $g^{Ih}(T, p)$, or IAPWS-06 formulation (Feistel
225   and Wagner 2006), see Tables A2 and A3 of Appendix A, depending on pressure p.

227   (iii)   A Gibbs function of *IAPSO Standard Seawater*, $g^{SW}(S, T, p)$, or IAPWS-08 formulation
228   (Feistel 2008a), see Tables A2 and A3 of Appendix A. The variable S, at which a subscript
229   A is omitted here for simplicity, is the specific or *Absolute Salinity*, the mass fraction of
230   dissolved salt in seawater, which differs from *Practical Salinity*, S_P, measured by present-
231   day oceanographic instruments, as well as from various other obsolete salinity scales
232   (Millero et al. 2008). Throughout this paper, the term "salinity" is exclusively short hand
233   for TEOS-10 Absolute Salinity. Sea salt is assumed to have stoichiometric *Reference
234   Composition*. The pure-water limit, $g^{SW}(0, T, p) = g^W(T, p)$, is the Gibbs function of
235   liquid water computed from the IAPWS-95 Helmholtz function $f^W(T, \rho)$. For brackish
236   seawater, g^{SW} has implemented Debye's root law of dilute electrolyte solutions (Landau
237   and Lifschitz 1966, Falkenhagen et al. 1971).

239   (iv)   A Helmholtz function of humid air, $f^{AV}(A, T, \rho)$, or IAPWS-10 formulation (Feistel et al.
240   2010a), see Tables A1 and A2 of Appendix A. The variable A is the mass fraction of dry air
241   admixed with water vapour, so that $q = 1 - A$ is the *specific humidity*. The dry-air limit
242          $f^{AV}(1, T, \rho) = f^A(T, \rho)$ equals, up to modified reference-state conditions, the equation
243   of state of Lemmon et al. (2000). The air-free limit $f^{AV}(0, T, \rho) = f^V(T, \rho)$ equals the
244   IAPWS-95 Helmholtz function of water vapour. In f^{AV}, the interaction of water vapour
245   with dry air is described by 2nd and 3rd virial coefficients.

248   Thermodynamic potentials include certain adjustable constants expressing the absolute energies and
249   entropies of the particular substances, which are not available from measurement (Planck 1906,
250   Feistel 2019b) and have, in turn, no effect on measurable properties derived from those potentials.
251   In fact, among the comprehensive experimental data sets from which the TEOS-10 equations were
252   derived, none of those are suitable for fitting the empirical coefficients that represent absolute
253   energies and entropies of those equations. For this reason, the International Conference on the
254   Properties of Steam at London defined in 1967 the common triple point of water as the reference
255   state at which those absolute values were arbitrarily set. Since then, no evidence has appeared for
256   putative conflicts caused by such settings with any technical or scientific applications of the
257   equations. Despite this, Feistel and Wagner (2006) and Feistel et al. (2008b) discuss the
258   implementation of alternative residual entropies of water, if that should be of interest in exceptional

259 applications of TEOS-10. For recent discussions of Pauling's absolute "residual" entropy at zero kelvin
260 and Nernst's Third Law of thermodynamics, see Kozliak and Lambert (2008), Gutzow and Schmelzer
261 (2011), Takada et al. (2015), Schmelzer and Tropin (2018), Feistel (2019b), or Shirai (2023).

263 The TEOS-10 reference states (Feistel et al. 2008b, 2010a) are the triple point of water, $T_{\text{TP}} = $
264 273.16 K, $p_{\text{TP}} = 611.654\,771$ Pa, where the conditions

266 $$\eta_{\text{TP}}^{\text{W}} = 0, \qquad e_{\text{TP}}^{\text{W}} = 0, \tag{1}$$

268 are imposed, and the standard ocean state at Absolute Salinity, $S_{\text{SO}} = 35.165\,04$ g kg^{-1}, absolute
269 temperature, $T_{\text{SO}} = 273.15$ K, and absolute pressure, $p_{\text{SO}} = 101\,325$ Pa, with the conditions for sea
270 salt,

272 $$\eta_{\text{SO}}^{\text{SW}} = 0, \qquad h_{\text{SO}}^{\text{SW}} = 0, \tag{2}$$

274 and for dry air,

276 $$\eta_{\text{SO}}^{\text{A}} = 0, \qquad h_{\text{SO}}^{\text{A}} = 0. \tag{3}$$

278 Here, η, e and h, respectively, are specific entropy, internal energy and enthalpy of water
279 (superscript W), seawater (superscript SW) and dry air (superscript A). The TEOS-10 potential
280 functions and properties derived thereby are numerically implemented in two different libraries, the
281 Sea-Ice-Air (SIA) and the Gibbs-Seawater (GSW) libraries, see Table A4 in Appendix A.

283 The SIA library includes empirical coefficients only in the four fundamental potentials (Feistel 2010d,
284 Wright et al. 2010). All other potential functions and properties are derived strictly by mathematical
285 operations to ensure consistent results, even at the cost of low computation speeds as a result of
286 stacked iteration procedures. All quantities are exclusively expressed in basic SI units such as kg, m, J
287 or Pa. A more recent extension of SIA code is reported in Feistel et al. (2022) for the computation of
288 relative fugacity.

290 The GSW library is tailored for oceanographic models, optimised in computation speed (Roquet et al
291 2015). For fast numerical evaluation, GSW procedures contain new empirical coefficients determined
292 from the SIA library functions by regression. Units and variables are adjusted to common
293 oceanographic practice such as pressure in decibars relative to surface pressure, or temperatures in
294 °C. *Conservative Temperature* (CT) is used as a new preferred thermal variable. An additional
295 thermodynamic potential has been constructed (McDougall et al. 2023) that supports the use of CT
296 universally as an independent variable.

298 **3   Potential Enthalpy and Ocean Heat Content (OHC)**

299 Thermodynamically, the term "Ocean Heat Content" (OHC) is a sloppy wording. "Content" means a
300 state quantity of a body or volume while, by contrast, "heat" is an exchange quantity rather than a
301 state quantity. "We have … a right to speak of heat as a *measurable quantity*, … however, … we have
302 no right to treat heat as a *substance*" (Maxwell 1888: p. 7). "The obsolete hypothesis of heat being a
303 substance is excluded" (Sommerfeld 1988: p. 6). "Heat is not a substance! More formally: Heat is not
304 a thermodynamic function of state" (Romer 2001: p. 107). This distinction is qualitatively
305 fundamental (Feistel 2023). Physical conservation quantities such as energy or mass have the key

306 property that the change of that quantity in a volume equals the flux of that quantity across the
307 boundary (Landau and Lifschitz 1966, Glansdorff and Prigogine 1971), but this does not apply to
308 "heat". For example, a heat engine receives a permanent net heat flux without getting permanently
309 hotter. While asking how much "heat" is contained in the ocean may find ambiguous answers, it is
310 well defined to say how much heat has entered or left the ocean across its boundary by a specified
311 process that transfers the ocean from a certain state of reference to the current state of interest. In
312 this section, based upon TEOS-10, related states and processes are described which may properly
313 specify what is commonly termed OHC. This consideration intrinsically connects OHC with ocean-
314 atmosphere exchange processes relevant for climate change.

315 Since a long time, measuring and calculating the ocean's "heat" has been a question of central
316 interest to oceanography. Recently, this issue has become even more important and urgent in the
317 context of climate change. "The total energy imbalance at the top of atmosphere is best assessed by
318 taking an inventory of changes in energy storage. The main storage is in the ocean" (Abraham et al.
319 2013: p. 450). The conventional approach is a formally defined mathematical procedure based on
320 potential temperatures. "Changes to ocean heat content (OHC) can be calculated from
321 measurements of the temperature evolution of the ocean. The OHC is attained from the difference
322 of the measured potential temperature profile and the potential temperature climatology. This
323 difference is integrated over a particular reference depth (for instance, 700 m) and is multiplied by a
324 constant ocean density reference and heat capacity" (Abraham et al. 2013: p. 468). However, in
325 representing a kind of "heat substance", this OHC definition has no rigorous thermodynamic
326 justification, and the relation to processes of ocean-atmosphere heat fluxes is not entirely clear. If a
327 sea-air heat flux of 1 W m^{-2} warms up the atmosphere, by what rate exactly will that OHC decrease?

328 Making the seawater properties entropy and enthalpy quantitatively available, TEOS-10 has offered a
329 thermodynamically improved option for defining OHC (McDougall et al. 2021), in the form of the
330 integral over the ocean volume,

331 $$OHC = \int h^{\mathrm{SW}}(S, \eta, p_0) \, \rho^{\mathrm{SW}}(S, \eta, p) \mathrm{d}V \,. \tag{4}$$

332 Here, $h^{\mathrm{SW}}(S, \eta, p_0)$ is the *potential enthalpy* (McDougall 2003) relative to the surface pressure, p_0,
333 and $\rho^{\mathrm{SW}}(S, \eta, p)$ is the in-situ mass density at the pressure p of a parcel with salinity and entropy
334 equal to those before. This definition can be understood in terms of both, a specified process of heat
335 exchange, and a reference state relative to which OHC is counted, as follows (Feistel 2024):

336 (i) A virtual **heat exchange process** supporting the definition (4) is sketched in Fig. 6. In turn,
337   each ocean parcel with in-situ properties (S, η, p) is lifted to the surface pressure p_0,
338   keeping its salinity and entropy constant. There, it reversibly exchanges heat, $\mathrm{d}h = T\mathrm{d}\eta$,
339   with a measuring device until the parcel's entropy has reached a certain reference value,
340   η_{ref}, while the parcel's salinity remains unchanged. Subsequently, the heat is reversibly
341   put back to the parcel which is then returned to its original location. The work required
342   to lift and lower the parcel is balanced because the parcel's thermodynamic state is
343   exactly the same before and after the balanced reversible heat exchange across the
344   surface. The "heat content" defined this way for a single parcel is added up then over all
345   ocean parcels to result in its total OHC value.
346 (ii) The **reference state** relative to which OHC is measured may freely be specified at will,
347   but beneficially be chosen with respect to its convenience or usefulness. In the case of
348   eq. (4), the OHC reference state is zero potential enthalpy (or zero Conservative
349   Temperature, McDougall 2003) of all ocean parcels.

350 The process depicted in Fig. 6 measures the total heat flux $\int dh = \int T d\eta$ which changes the entropy
351 of the given sample from the current value, η, to some arbitrary reference value, η_{ref}, and this way,
352 the process also changes the parcel's enthalpy from $h^{\text{SW}}(S, \eta, p_0)$ to $h^{\text{SW}}(S, \eta_{\text{ref}}, p_0)$. Integration
353 over all ocean samples results in an OHC value of

354 $$OHC^* = \int \left[h^{\text{SW}}(S, \eta, p_0) - h^{\text{SW}}(S, \eta_{\text{ref}}, p_0) \right] \rho^{\text{SW}}(S, \eta, p) dV. \qquad (5)$$

355 While the choice of the OHC reference state is - in principle - entirely arbitrary, such as simply putting
356 $\eta_{\text{ref}} = 0$, it is reasonable to better adapt this selection to the purpose of the OHC definition. The
357 main purpose of estimating OHC is keeping track of the ocean's long-term energy balance, in
358 particular of the ocean's share of global warming. Three conditions appear immediately plausible in
359 order to achieve this goal,

360 (i) *The OHC definition should ensure that OHC differences represent a suitable spatial*
361 *integral over the heat fluxes crossing the ocean's boundaries.* As discussed in more detail
362 in Section 5.3, production of entropy, $d_i\eta$, caused by irreversible processes between
363 different parcels within the ocean, does not affect the ocean's total enthalpy budget.
364 This is quite in contrast to entropy exchange, $d_e\eta$, of the given sample in the form of
365 reversible heat flux across its boundary. Such irreversible processes affect the ocean's
366 total potential enthalpy much less than its total entropy (McDougall et al. 2021). For this
367 reason the OHC reference state should explicitly be defined in terms of potential
368 enthalpy, $h^{\text{SW}}(S, \eta_{\text{ref}}, p_0)$, and this way only implicitly in terms of entropy by specifying
369 $\eta_{\text{ref}}(S)$.

370
371 (ii) *Provided that the ocean's mass remains the same between any two ocean states (1) and*
372 *(2), the difference OHC(1) – OHC(2) should depend only on the surface heat flux balance*
373 *during the time in between. In particular, differences OHC(1) – OHC(2) should not depend*
374 *on the OHC reference state.* For this reason, the OHC reference value should be
375 independent of changes occurring in the density distribution, $\rho^{\text{SW}}(S, \eta, p)$. This can be
376 achieved by assigning to each ocean parcel the same reference potential enthalpy,
377 $h^{\text{SW}}(S, \eta_{\text{ref}}, p_0) = \text{const}$, even though such a state may hardly ever be observed in the
378 real ocean.

379
380 (iii) *Quantitatively, OHC values estimated at different times or places should be mutually*
381 *comparable without estimation bias resulting from possibly changing methods of OHC*
382 *calculation.* For this reason, resulting OHC values should be independent of the inevitable
383 arbitrary, physically irrelevant reference-state conditions imposed on energy and
384 entropy, such as eqs. (1)-(3). This can be achieved by assigning to each ocean parcel the
385 same standard-ocean enthalpy as its reference potential enthalpy, $h^{\text{SW}}(S, \eta_{\text{ref}}, p_0) =$
386 h_{SO}. In the special case of TEOS-10 enthalpy, this value is defined by eq. (2), $h_{\text{SO}} = 0$.
387 This choice is implicitly made by the definition (4) but needed to be considered explicitly
388 as soon as alternative equations for seawater enthalpy or entropy are employed, such as
389 those of Millero and Leung (1976) and Millero (1982, 1983).

390
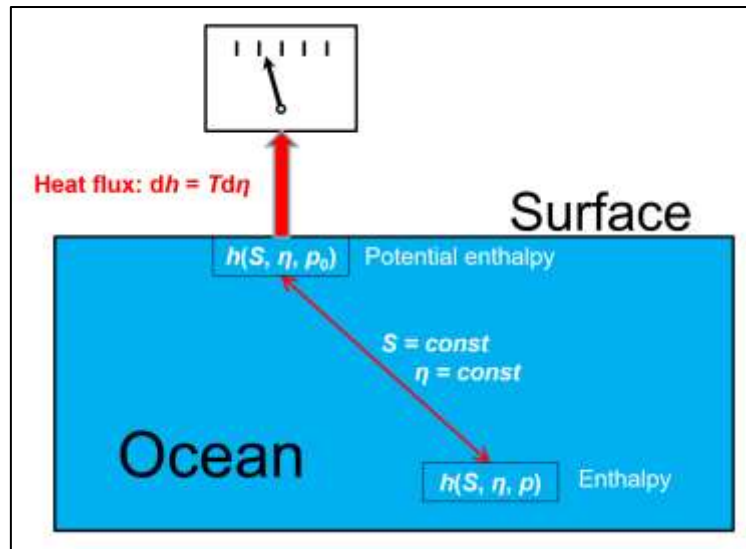
Fig. 6: Schematic of a conceptual process defining the ocean heat "content" (OHC) by measuring heat flux across the ocean boundary according to eqs. (4) and (5).

In a sense consistent with the previous OHC definition (Abraham et al. 2013), also a climatological average state could in principle be chosen as the OHC reference. However, this option includes the problem that the salinity distribution of the current ocean may differ from the reference ocean, and that thermodynamically properly treating the required salt exchange processes at the surface may turn the issue unnecessarily complicated. A detailed comparison of the OHC definition (4) with its precursor prior to TEOS-10 is provided by McDougall et al. (2021). OHC as a part of the total energy balance of the ocean is analysed by Tailleux (2010, 2018) and Tailleux and Dubos (2024).

4   Relative Fugacity and Ocean Evaporation Rate

"The global water cycle and the exchange of freshwater between the atmosphere and ocean is poorly understood. … It has been predicted that increasing global temperatures will lead to an enhanced global water cycle" (Holliday et al. 2011: p. 34). In the past, several climate researchers have argued that along with global warming the marine evaporation has or will be "amplified" or "intensified" (Feistel and Hellmuth 2021). However, it was not always made clear whether this may mean that (a) in the course of a year, more water vapour is transferred from the global ocean to the atmosphere, or (b) that the global mean evaporation rate remains unchanged while locally or temporally, evaporation is more intense, or (c) any combination of the two variants. Conclusions of kind (a) were drawn by renowned climatologists such as Budyko (1984), Flohn et al. (1992), Yu (2007), Randall (2012), Francis (2021) or Zhang et al. (2021).

By contrast, in favour of option (b), the currently observed ocean warming at a rate about 1 W m^{-2} does not support assumptions of an enhanced hydrological cycle with related latent-heat cooling, rather, it more likely suggests a slight reduction of evaporation. Two decades ago, Held and Soden (2006: p. 5687-5689) had already clearly stated that "it is important that the global-mean precipitation or evaporation, commonly referred to as the strength of the hydrological cycle, does not scale with Clausius–Clapeyron. … We can, alternatively, speak of the mean residence time of water vapor in the troposphere as increasing with increasing temperature." Subsequent observations have underpinned their statement.
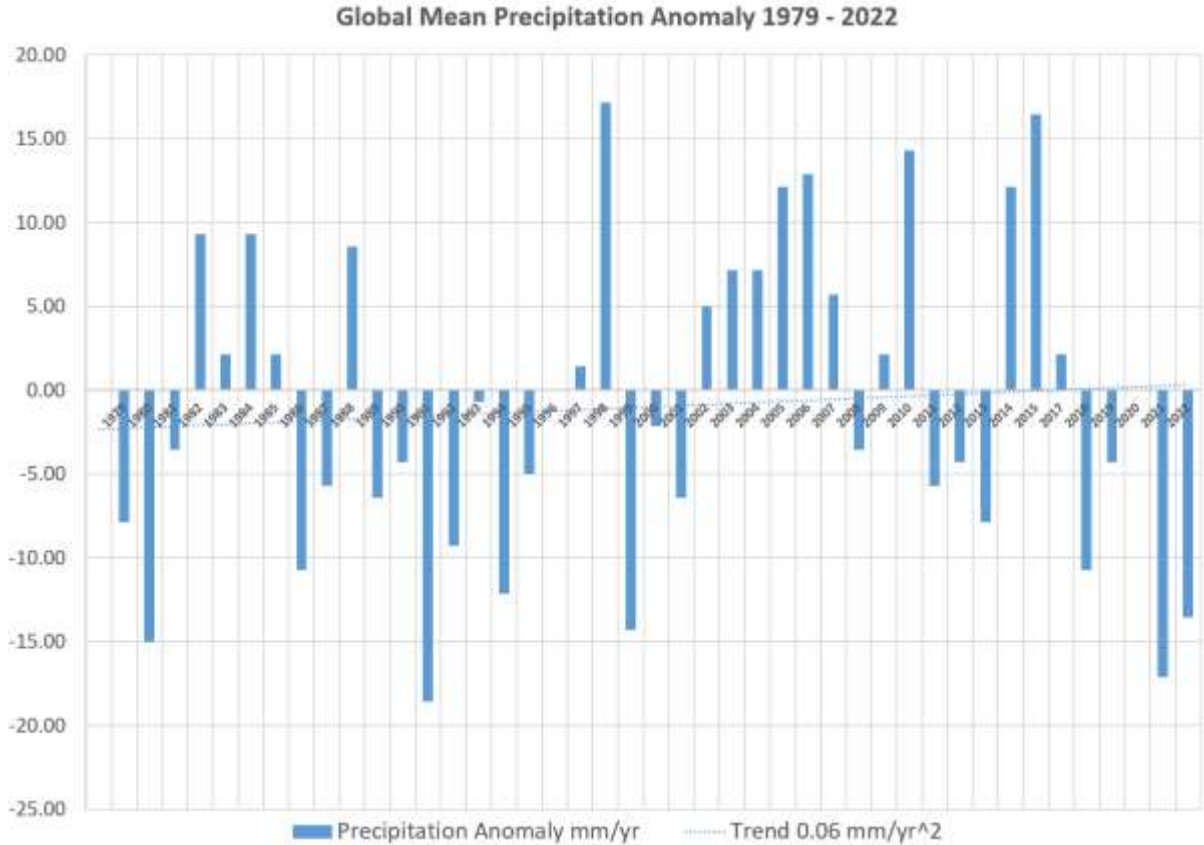
Fig. 7: Global mean precipitation anomaly 1979-2022 in mm yr^{-1}. The values displayed exhibit a minor increasing trend (dotted line) of 0.06 mm yr^{-2}. Data from Vose et al. (2023)

Between 1979 and 2022, annual mean global precipitation values, see Fig. 7, fluctuated by about ± 10 mm yr^{-1}, in particular due to La Niña events, but do not exhibit a significant long-term trend (Vose et al. 2023). Under the common assumption that global precipitation is balanced against evaporation, no substantial strengthening of the hydrological cycle may be observed yet.

Probably, the minor trend of 0.06 mm yr^{-2} of the data displayed in Fig. 7 is statistically insignificant. Associated with this apparent trend, the latent heat transferred to the troposphere can be estimated to a negligible putative warming rate of additional 0.5 mW m^{-2} per year, which could explain only 10 % of observed atmospheric warming by 1.7 °C per century (Morice et al. 2012, Feistel and Hellmuth 2021).

The thermodynamic driving force for evaporation is the difference between the chemical potentials of water in humid air and in seawater at the two sides of the sea-air interface (Kraus and Businger 1994). TEOS-10 has made this difference numerically available in the form of the water mass evaporation rate (Feistel and Hellmuth 2022, 2023)

$$J_{\mathrm{W}} = -D_f(u) \ln \frac{\psi_f}{x_{\mathrm{W}}}. \tag{6}$$

Here, x_{W} is the mole fraction of water in seawater. Consistent with Wüst (1920), for the standard ocean with Reference Composition, this fraction is (Millero et al. 2008: Table 4),

$$x_{\mathrm{W}} = \frac{53.556\,514\,4}{54.676\,283\,8} = 0.979\,52, \qquad \ln x_{\mathrm{W}} = -0.0206926. \tag{7}$$

443   In eq. (6), $D_f(u)$, the *Dalton coefficient*, is an empirical transfer coefficient as a function of the wind
444   speed, u, as a parameterisation of the turbulent transport processes of water in the vicinity of the
445   interface. Applications of the *Monin-Obukhov Similarity Theory* (MOST) in order to estimate the
446   Dalton coefficient are reviewed by Liu et al. (1979), Foken and Richter (1991), Foken (2004, 2016) and
447   in the Digital Supplement of Feistel and Hellmuth (2024). A review of empirical Dalton coefficients is
448   given by Debski (1966); historical evaporation experiments are summarised by Biswas (1969).

449   In eq. (6), the sea-surface humidity is expressed by the *relative fugacity* (RF), ψ_f, defined by the ratio
450   of the water-vapour fugacity in humid air, f_V, to that fugacity at saturation, f_V^{sat} (Feistel and Lovell-
451   Smith 2017), see eq. (49). In ideal-gas approximation, RF equals conventional RH (Lovell-Smith et al.
452   2016)

453    $$\psi_f \equiv \frac{f_V}{f_V^{sat}} \approx \psi_x \equiv \frac{x}{x^{sat}}. \tag{8}$$

454   Here, the mole fraction of water vapour in humid air is x, and its value at saturation is x^{sat}. Further,
455   ψ_x is the conventional definition of RF in metrology and meteorology which, however, is inconsistent
456   with alternative definitions such as the one employed in climatology (Lovell-Smith et al. 2016).
457   Independent of ideal-gas conditions, but sufficiently close to saturation, such as near the sea surface,
458   RF can be estimated in excellent approximation from the Clausius-Clapeyron formula (Feistel et al.
459   2022),

460    $$\psi_f \approx \exp\left\{ \frac{L(T_{dp}, p)}{R_W} \left(\frac{1}{T} - \frac{1}{T_{dp}} \right) \right\}. \tag{9}$$

461   The evaporation enthalpy of pure water (IAPWS SR1-86 1992) at the dewpoint T_{dp} is L, and $R_W =$
462    $461.523 \text{ J kg}^{-1}\text{ K}^{-1}$ is the specific gas constant of water. The typical marine RF is

463    $$\psi_f \approx 80 \text{ \%rh}, \tag{10}$$

464   and is fairly independent of region, season or global warming (Dai 2006, Randall 2012, Rapp 2014,
465   MetOffice 2020). Indeed, observed ocean surface RH has no significant climatological trend (Willett
466   et al. 2023). Similarly, observed ocean wind speeds seem to be unaffected by global warming (Azorin-
467   Molina et al. 2023). Eq. (6) for the evaporation rate depends only on wind speed and RF, so that it
468   may be concluded that also the global mean evaporation rate has no significant climatic trend. In
469   turn, as far as the release of latent heat is the main driving force of marine tropospheric dynamics,
470   without increase of that release the mean wind speed is not expected to grow. "Latent heat is the
471   main fuel that powers hurricanes, thunderstorms and normal bouts of lousy weather" (Francis 2021).
472   Hence, the TEOS-10 approach in the form of eq. (6) appears to be consistent with the prediction of
473   Held and Soden (2006) that the global evaporation does not increase along with temperature.

474   Various empirical evaporation equations, commonly known as *Dalton equations*, are found in the
475   literature (Wüst 1920, Sverdrup 1936, 1937, Montgomery 1940, Debski 1966, Biswas 1969,
476   Baumgartner and Reichel 1975). Several numerical climate models estimate evaporation from the
477   formula (Stewart 2008, Pinker et al. 2014),

478    $$J_W = D_q(u)(q_0 - q_{10}), \tag{11}$$

479   where q_0 is the specific humidity at the sea surface and q_{10} is that at 10 m height, or from (Josey et
480   al. 1999, 2013)

481    $$J_W = D_q(u)(0.98\, q^{sat} - q). \tag{12}$$

482   Here, q is the near-surface specific humidity, and q^{sat} is the saturation value at the same
483   temperature and pressure. The factor 0.98 accounts for the salinity, see eq. (7). After a few

484   approximation steps (Feistel and Hellmuth 2023), these Dalton equations can be derived from the

485   TEOS-version, eq. (6), however, there is an important qualitative difference. At constant RH, due to

486   global warming, specific humidities such as q and q^{sat}, as well as their difference, are increasing

487   following the Clausius-Clapeyron saturation formula. Accordingly, eq. (12) implies that also the

488   evaporation rate J_{W} is growing this way, by contrast to eq. (6). This virtual acceleration of the

489   hydrological cycle is evidently inconsistent with the prediction of Held and Soden (2006). This

490   parameterisation-caused additional latent heat flux implies a spurious ocean cooling that may

491   contribute to the finding that many numerical climate models tend to underestimate the observed

492   ocean warming (Weller et al. 2022).

493   From eq. (6), the sensitivity of the latent heat flux, LJ_{W}, with respect to RH variations is easily

494   estimated. For a mean evaporation rate of 1200 mm per year, the corresponding mass flux is about

495    $J_{\text{W}} \approx 3.8 \times 10^{-5} \text{ kg m}^{-2}\text{s}^{-1}$ and the related heat flux is $LJ_{\text{W}} \approx 95 \text{ W m}^{-2}$ with respect to the ocean

496   surface area and a specific evaporation enthalpy of $L = 2\,501 \text{ kJ kg}^{-1}$. At a surface humidity of $\psi_f =$

497   0.8, a value of $D_f(u) \approx 1.87 \times 10^{-4} \text{ kg m}^{-2}\text{s}^{-1}$ can be concluded for the mass transfer coefficient,

498   and of $LD_f(u) \approx 468 \text{ W m}^{-2}$ for that of latent heat. Then, from

499    $$\Delta(LJ_{\text{W}}) = L \frac{\partial J_{\text{W}}}{\partial \psi_f} \Delta\psi_f = -LD_f(u) \frac{\Delta\psi_f}{\psi_f} \tag{13}$$

500   it follows that an increase by $\Delta\psi_f = 1 \text{ \%rh}$ results in a heat flux reduction by $\Delta(LJ_{\text{W}}) =$

501   5.85 W m^{-2}. So, the currently observed ocean warming (Cheng et al. 2024) of 1.3 W m^{-2} could

502   theoretically be caused already by a minor marine humidity increase of $\Delta\psi_f = 0.2 \text{ \%rh}$, a value far

503   below the present measurement uncertainty between 1 and 5 %rh of relative humidity. The

504   resolution of climate models and observation seems to be insufficient yet to identify the possible role

505   of RH for the unclear explanation of the warming ocean.

506

507   **5   Sea Air as a Two-Phase Composite**

508   Gibbs' (1873) method of using potential functions can be applied to any systems possessing stable

509   thermodynamic equilibria and obeying energy conservation, without being restricted to merely

510   homogeneous or single-phase samples. The intentionally strict mutual consistency of the different

511   TEOS-10 potential functions permits a mathematical description of multi-phase composites such as

512   sea ice, consisting of ice with included brine pockets (Feistel and Hagen 1998, Feistel and Wagner

513   2005), or clouds, where liquid water or ice is floating in saturated humid air (Hellmuth et al. 2021).

514   Another important model is that of *sea air*, a sample consisting of a mass m^{SW} of seawater in

515   thermodynamic equilibrium with a mass m^{AV} of humid air (Feistel et al. 2010d, Feistel and Hellmuth

516   2023). Such a model may serve as a mathematical description for certain thermodynamic properties

517   of ocean-atmosphere interaction.

518   Extensive thermodynamic functions such as Gibbs energy or enthalpy are additive with respect to the

519   two separate phases of the sample. Equilibrium between those parts requires equal temperatures

520   and pressures. For this reason, a Gibbs function of sea air is an appropriate potential for the

521   composite system with the TEOS-10 Gibbs functions $g^{\text{SW}}(S, T, p)$ describing the liquid part and

522    $g^{\text{AV}}(A, T, p)$ the gas part. Let the masses of the substances in the parts be m^{W} of liquid water, m^{S} of

523   dissolved salt, m^{A} of dry air and m^{V} of water vapour. Note that TEOS-10 neglects solubility of dry air

524   constituents in liquid water. From combinations of the partial masses follow the liquid mass, $m^{\text{SW}} =$

525    $m^{\text{S}} + m^{\text{W}}$, the gas mass, $m^{\text{AV}} = m^{\text{A}} + m^{\text{V}}$, the total mass $m = m^{\text{SW}} + m^{\text{AV}}$, the total water mass

526    $m^{\text{WV}} = m^{\text{W}} + m^{\text{V}}$, the salinity $S = m^{\text{S}}/m^{\text{SW}}$ and the dry-air fraction $A = 1 - q = m^{\text{A}}/m^{\text{AV}}$.

527   The Gibbs energies of the two phases of sea air are additive,

528 $$G^{\mathrm{SA}} = G^{\mathrm{SW}} + G^{\mathrm{AV}} = mg^{\mathrm{SA}}\,,\tag{14}$$

529 and, accordingly, the Gibbs function of sea air, g^{SA}, may be constructed from that of seawater,
530 $g^{\mathrm{SW}}(S,T,p)$, with a liquid mass fraction of $w^{\mathrm{SW}} = m^{\mathrm{SW}}/m$ and that of humid air, $g^{\mathrm{AV}}(A,T,p)$, with
531 a gaseous mass fraction of $w^{\mathrm{AV}} = m^{\mathrm{AV}}/m = 1 - w^{\mathrm{SW}}$,

532 $$g^{\mathrm{SA}}(S,A,w^{\mathrm{SW}},T,p) = w^{\mathrm{SW}}g^{\mathrm{SW}}(S,T,p) + (1 - w^{\mathrm{SW}})g^{\mathrm{AV}}(A,T,p).\tag{15}$$

533 If the two phases are assumed to be at mutual equilibrium, they possess the same temperature,
534 pressure and chemical potentials, see eq. (B.11) in Appendix B, $\mu_{\mathrm{W}}^{\mathrm{SW}} = \mu_{\mathrm{V}}^{\mathrm{AV}}$, namely that of water in
535 seawater,

536 $$\mu_{\mathrm{W}}^{\mathrm{SW}}(S,T,p) = g^{\mathrm{SW}} - S\left(\frac{\partial g^{\mathrm{SW}}}{\partial S}\right)_{T,p},\tag{15}$$

537 equalling that of water vapour in humid air,

538 $$\mu_{\mathrm{V}}^{\mathrm{AV}}(A,T,p) = g^{\mathrm{AV}} - A\left(\frac{\partial g^{\mathrm{AV}}}{\partial A}\right)_{T,p}.\tag{16}$$

539

540 ### 5.1 Sea Air as a Model for Latent Heat of Evaporation

541 Water evaporated from the ocean surface drives the climate system. "The by far largest part of heat
542 conveyed to the air is in the form of latent heat during subsequent condensation along with cloud
543 formation. The heat budget over the sea is mainly controlled by the latent heat released to the air"
544 (Albrecht 1940). It is the "*heat source for a gigantic steam engine*", as Heinrich Hertz had put it in his
545 1885 inaugural lecture at Karlsruhe (Mulligan and Hertz 1997). The latent heat of evaporation of pure
546 liquid water into pure water vapour is numerically well known from experiments (IAPWS SR1-86
547 1992, Harvey 1998, Wagner and Pruß 2002). Slightly differing values are reported in various
548 textbooks on hydrology (Debski 1966: p. 332), meteorology (Linke and Baur 1970) or geophysics (Gill
549 1982, Kraus and Businger 1994). TEOS-10, however, permits the computation of evaporation
550 properties from seawater into humid air, based on the first-time availability of standard equations
551 for enthalpies and chemical potentials of those non-ideal mixtures.
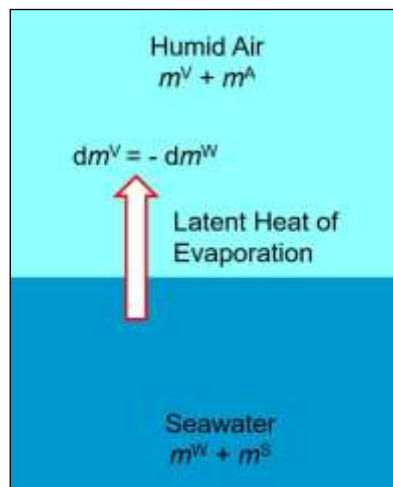
552

553 Fig. 8: Conceptual thermodynamic "sea air" model of ocean-atmosphere interaction as a two-phase
554 composite of seawater and humid air

555

556 "Latent heat is the quantity of heat which must be communicated to a body in a given state in order
557 to convert it into another state without changing its temperature" (Maxwell 1888: p.73). If an
558 infinitesimal amount of water is transferred from the liquid to the gas phase (Fig. 8), while
559 temperature and pressure remain at their equilibrium values, and the total masses of salt, m^S, dry
560 air, m^A, and water, m^{WV}, are not affected, the isobaric-isothermal latent heat of evaporation may be
561 defined by

562 $$L^{SA} \equiv \left(\frac{\partial H^{SA}}{\partial m^V} \right)_{T,p,m^S,m^A,m^{WV}}. \tag{17}$$

563 This latent heat accounts for the loss of total heat of the sea-air sample associated with the loss of
564 liquid water and equal gain of water vapour,

565 $$\frac{\partial m^V}{\partial T} = -\frac{\partial m^W}{\partial T}. \tag{18}$$

566 Here, H^{SA} is the enthalpy of sea air, available from the Gibbs function (15) through the sum

567 $$H^{SA} \equiv m^{SW} h^{SW} + m^{AV} h^{AV}. \tag{19}$$

568 Here, the specific enthalpies of seawater,

569 $$h^{SW} = g^{SW} - T \left(\frac{\partial g^{SW}}{\partial T} \right)_{S,p}, \tag{20}$$

570 and of humid air,

571 $$h^{AV} = g^{AV} - T \left(\frac{\partial g^{AV}}{\partial T} \right)_{A,p}, \tag{21}$$

572 are defined in terms of the related Gibbs functions.
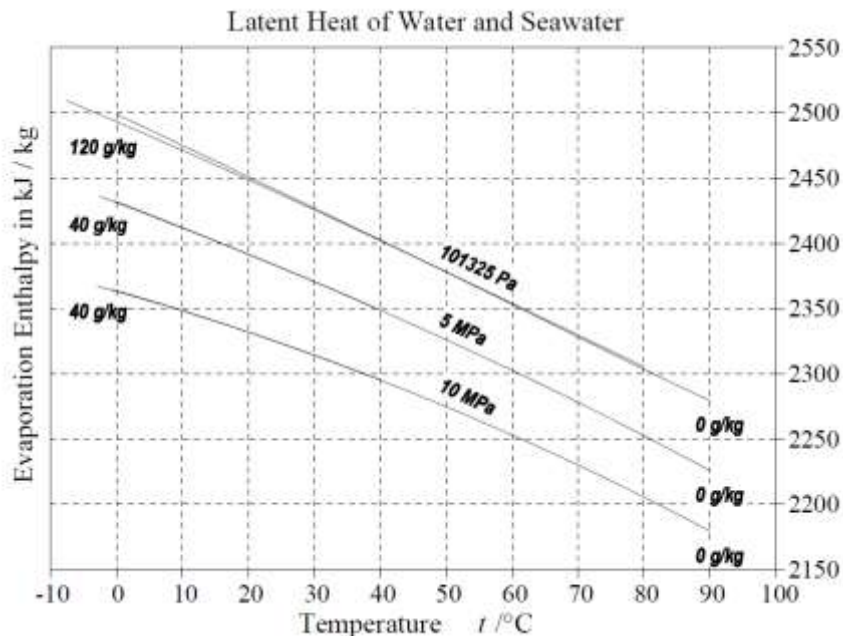
573

574 Fig. 9: Evaporation enthalpy, eq. (23), of seawater in equilibrium with humid air at different
575 temperatures, pressures and salinities. The dependence on salinity is very weak; graphically, the
576 related curves are hardly distinguishable. The nonlinear dependence on temperature is more
577 pronounced at elevated pressures. Figure from Feistel et al. (2010a: p. 105)

578

579 The derivative (17) is carried out in the form

580 $$L^{\text{SA}} = -h^{\text{SW}} - m^{\text{SW}} \left(\frac{\partial h^{\text{SW}}}{\partial S}\right)_{T,p} \left(\frac{\partial S}{\partial m^{\text{V}}}\right)_{m^{\text{S}},m^{\text{WV}}} + h^{\text{AV}} + m^{\text{AV}} \left(\frac{\partial h^{\text{AV}}}{\partial A}\right)_{T,p} \left(\frac{\partial A}{\partial m^{\text{V}}}\right)_{m^{\text{A}}} , \qquad (22)$$

581 which results in the TEOS-10 latent-heat equation (Feistel et al. 2010a, Feistel and Hellmuth 2023),

582 $$L^{\text{SA}} = h^{\text{AV}} - A \left(\frac{\partial h^{\text{AV}}}{\partial A}\right)_{T,p} - h^{\text{SW}} + S \left(\frac{\partial h^{\text{SW}}}{\partial S}\right)_{T,p} , \qquad (23)$$

583 with typical values shown in Fig. 9. If seawater is in mutual equilibrium with humid air at given
584 temperature and pressure, salinity and humidity of the parts of sea air satisfy the condition $\mu_{\text{W}}^{\text{SW}} =$
585 $\mu_{\text{V}}^{\text{AV}}$, given by eqs. (15) and (16),

586 $$\Delta\mu \equiv g^{\text{SW}} - S \left(\frac{\partial g^{\text{SW}}}{\partial S}\right)_{T,p} - g^{\text{AV}} + A \left(\frac{\partial g^{\text{AV}}}{\partial A}\right)_{T,p} = 0 \qquad (24)$$

587 At given masses of salt, m^{S}, of dry air, m^{A}, and of total water, $m^{\text{WV}} = m^{\text{W}} + m^{\text{V}}$, eq. (24) controls
588 the value of either m^{W} or m^{V}, and this way also of S and A as functions of $T, p, m^{\text{S}}, m^{\text{A}}$ and m^{WV}.
589 Related numerical solutions are readily implemented in the TEOS-10 SIA library; the latent heat of
590 sea air can be computed by calling the function sea_air_enthalpy_evap_si(), see Wright et al.
591 (2010).

592 Latent heat of eq. (23) is valid regardless of the equilibrium condition, eq. (24), being satisfied or not.
593 The non-equilibrium case is considered separately in Section 5.3.

594

595 *5.2 Sea Air as a Model of Sea Spray*

596 As a special form of air-sea interaction, sea spray is typically ejected from the crest of a breaking
597 wave, which may happen all along oceanic coasts but also wherever whitecaps are produced from
598 swell or stormy sea state, see Fig. 10. In contrast to fresh-water haze, droplets of sea spray cannot
599 completely evaporate for the salt they contain, and rather develop into a floating persistent Köhler
600 (1936) equilibrium between droplet size, droplet salinity and ambient relative fugacity (Hellmuth and
601 Shchekin 2015, Pöhlker et al. 2023). This equilibrium can be described by the TEOS-10 model of sea
602 air if the additional Kelvin pressure caused by the surface tension is allowed for.

603 In the infrared spectral range, sea spray as well as other aerosols (Carlon 1970, 1980) may be
604 considered as a black absorber and emitter of thermal radiation. The resulting "gray atmosphere" is a
605 conveniently simple conceptual model for the long-wave radiative effects of dust or haze in the
606 climate system (Emden 1913). When heated from below, as in the case of the clear-sky marine
607 troposphere, a theoretical finding is that the thermally stratified gray troposphere exhibits a special
608 critical value of the isobaric heat capacity at $c_p = 4R$ (Pierrehumbert 2010: p. 201), R being the
609 molar gas constant. Vertical stability may be lost at $c_p > 4R$ and turbulent mixing is expected to
610 commence (Feistel 2011b: eq. 58 therein). Such a kinetic phase transition could substantially modify
611 the thermal radiation balance between troposphere and ocean surface.

612

613   Fig. 10: Sea spray ejection from a breaking wave crest of Atlantic swell. Photo taken at Cabo Trafalgar
614   in March 2011.

615

616   The terrestrial atmosphere is dominated by the two-atomic gases N_2 and O_2 with heat capacities
617   about $3.5\ R$ which prevent the putative radiative vertical instability to occur. This situation may
618   change, however, in the presence of haze or sea spray. To investigate this effect theoretically, in this
619   section a TEOS-10 equation for the heat capacity of equilibrium sea air is derived from the definition

620   $$c_p^{SA} \equiv \frac{1}{m}\left(\frac{\partial H^{SA}}{\partial T}\right)_{p,m^S,m^A,m^{WV}}. \tag{25}$$

621   The enthalpy of sea air is given by eq. (19). Taking into account water conservation upon
622   evaporation, $m^{WV} = $ const, that is,

623   $$\frac{\partial m^V}{\partial T} = -\frac{\partial m^W}{\partial T}, \tag{26}$$

624   and of eq. (23), the isobaric heat capacity of sea air is concluded to be

625   $$c_p^{SA} = w^{SW}c_p^{SW} + w^{AV}c_p^{AV} + L^{SA}\frac{1}{m}\frac{\partial m^V}{\partial T}. \tag{27}$$

626   To the additive contributions of the partial heat capacities of the liquid and the gas part, there
627   appears the latent heat of the water mass that evaporates from the liquid as vapour. This
628   evaporation rate is governed by the mutual equilibrium between seawater and humid air.

629   During the temperature change, sea-air equilibrium, eq. (24), is assumed to be maintained by water
630   transfer between the phases, changing S and A along with T,

631   $$\left(\frac{\partial \Delta\mu}{\partial T}\right)_{p,m^S,m^A,m^{WV}} = 0. \tag{28}$$

632   Carrying out the derivative, this condition reads

633   $$\left(\frac{\partial g^{SW}}{\partial T}\right)_{S,p} - S\left(\frac{\partial^2 g^{SW}}{\partial S \partial T}\right)_p - S\left(\frac{\partial^2 g^{SW}}{\partial S^2}\right)_{T,p}\left(\frac{\partial S}{\partial T}\right)_{m^S}$$

634
$$= \left(\frac{\partial g^{AV}}{\partial T}\right)_{A,p} - A \left(\frac{\partial^2 g^{AV}}{\partial A \partial T}\right)_p - A \left(\frac{\partial^2 g^{AV}}{\partial A^2}\right)_{T,p} \left(\frac{\partial A}{\partial T}\right)_{m^A}. \tag{29}$$

635 On the other hand, from combining eq. (23) with eq. (24) it follows that the latent heat may be
636 expressed by,

637
$$L^{SA} = T \left\{ \left(\frac{\partial g^{SW}}{\partial T}\right)_{S,p} - S \left(\frac{\partial^2 g^{SW}}{\partial S \partial T}\right)_p - \left(\frac{\partial g^{AV}}{\partial T}\right)_{A,p} + A \left(\frac{\partial^2 g^{AV}}{\partial A \partial T}\right)_p \right\}, \tag{30}$$

638 so that eq. (29) may be written as

639
$$L^{SA} = T \left\{ S \left(\frac{\partial^2 g^{SW}}{\partial S^2}\right)_{T,p} \left(\frac{\partial S}{\partial T}\right)_{m^S} - A \left(\frac{\partial^2 g^{AV}}{\partial A^2}\right)_{T,p} \left(\frac{\partial A}{\partial T}\right)_{m^A} \right\}. \tag{31}$$

640 Further, the total water mass balance, eq. (26), implies that

641
$$\left(\frac{\partial S}{\partial T}\right)_{m^S} = \left(\frac{\partial S}{\partial m^W}\right)_{m^S} \frac{\partial m^W}{\partial T} = \frac{S}{m^{SW}} \frac{\partial m^V}{\partial T}, \tag{32}$$

642 and similarly,

643
$$\left(\frac{\partial A}{\partial T}\right)_{m^A} = \left(\frac{\partial A}{\partial m^V}\right)_{m^A} \frac{\partial m^V}{\partial T} = -\frac{A}{m^{AV}} \frac{\partial m^V}{\partial T}. \tag{33}$$

644 Inserting those expressions into eq. (31), the equation for the isobaric evaporation rate of sea air is

645
$$\frac{\partial m^V}{\partial T} = \frac{L^{evap}}{T} \left\{ \frac{S^2}{m^{SW}} \left(\frac{\partial^2 g^{SW}}{\partial S^2}\right)_{T,p} + \frac{A^2}{m^{AV}} \left(\frac{\partial^2 g^{AV}}{\partial A^2}\right)_{T,p} \right\}^{-1}. \tag{34}$$
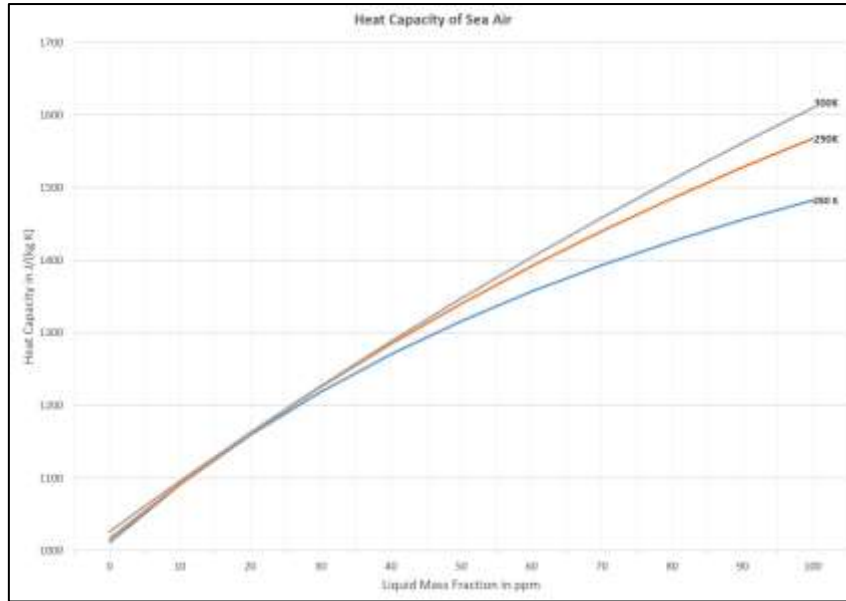
646

647 Fig. 11: TEOS-10 values for the isobaric specific heat capacity, eq. (35), of sea air at atmospheric
648 pressure and sea-spray standard-ocean salinity, S = 35.165 04 g kg^{-1}, at temperatures of 280 K (lower
649 curve), 290 K (middle curve) and 300 K (upper curve) as functions of the liquid mass fraction, w^{SW},
650 up to 100 ppm.

651

652 Together with eq. (34), the desired formula for the isobaric heat capacity (27) of sea air finally
653 becomes (Feistel et al. 2010a: eq. 6.22 therein),

654 $$c_p^{\text{SA}} = w^{\text{SW}}c_p^{\text{SW}} + \left(1 - w^{\text{SW}}\right)c_p^{\text{AV}} + \frac{\left(L^{\text{SA}}\right)^2}{T}\left\{\frac{S^2}{w^{\text{SW}}}\left(\frac{\partial^2 g^{\text{SW}}}{\partial S^2}\right)_{T,p} + \frac{A^2}{\left(1-w^{\text{SW}}\right)}\left(\frac{\partial^2 g^{\text{AV}}}{\partial A^2}\right)_{T,p}\right\}^{-1}. \quad (35)$$

655 Of the *liquid water content*, expressed in form of the liquid mass fraction, w^{SW}, realistic values may
656 typically range between 10^{-6} and 10^{-4} in the troposphere. Growing along with this fraction, related
657 heat capacities of sea air, eq. (35), may substantially exceed that of liquid-free humid air, c_p^{AV}, see
658 Fig. 11.

659

660 *5.3 Sea Air as a Model for Irreversible Evaporation*

661 The climate system functions far from thermodynamic equilibrium, permanently producing and
662 exporting entropy at an average rate about 1 W m^{-2} K^{-1} per global surface area (Ebeling and Feistel
663 1982, Feistel and Ebeling 2011). By contrast, TEOS-10 is a mathematical description of equilibrium
664 properties (Appendix B). The latter is applicable to states away from thermodynamic equilibrium
665 under the assumption of *local equilibrium* as introduced by Ilya Prigogine (1947, 1978). This
666 assumption means that spatially extended substances such as ocean or atmosphere consist of
667 sufficiently small volume elements that may reasonably be described as macroscopic equilibrium
668 states, homogeneous in temperature, pressure and chemical potentials. TEOS-10 thermodynamic
669 potentials can be used to describe those local states.

670 By definition, if a volume at equilibrium is divided into partial volumes, each of those parts is at
671 equilibrium itself, and each pair of those is at mutual equilibrium also. By contrast, the combination
672 of several local-equilibrium elements forms a non-equilibrium state if pairs of elements exist that are
673 out of mutual equilibrium. Extensive properties such as mass, energy, entropy or enthalpy can be
674 added up to give correct values of the entire system. When exchange processes between those
675 elements occur, gains and losses of masses, energies or enthalpies are mutually balanced by
676 conservation laws, however, this is not the case for entropy.

677 A tutorial case of a local equilibrium system may be the model of sea air (Feistel and Hellmuth 2024a)
678 depicted in Fig. 8. It consists of a mass $m^{\text{SW}} = m^{\text{S}} + m^{\text{W}}$ of seawater in contact with a mass $m^{\text{AV}} = $
679 $m^{\text{A}} + m^{\text{A}}$ of humid air. Both fluids are assumed to be at internal equilibrium themselves but not
680 necessarily in mutual equilibrium with one another. This is a natural geophysical situation – marine
681 RH has typical values of 80 %rh while the equilibrium of humid air with seawater, eq. (24), is
682 established at about 98 %rh. For simplicity, let all parts have equal temperatures and pressures.

683 If evaporation takes place, the partial water masses involved will change by a mass flux across the
684 sea surface,

685 $$J_m \equiv \frac{\mathrm{d}m^{\text{AV}}}{\mathrm{d}t} = \frac{\mathrm{d}m^{\text{V}}}{\mathrm{d}t} = -\frac{\mathrm{d}m^{\text{SW}}}{\mathrm{d}t} = -\frac{\mathrm{d}m^{\text{W}}}{\mathrm{d}t}. \quad (36)$$

686 The change of the total enthalpy of the sea-air sample is available from eqs. (17) and (23),

687 $$\frac{\mathrm{d}H^{\text{SA}}}{\mathrm{d}t} = \left(\frac{\partial H^{\text{SA}}}{\partial m^{\text{V}}}\right)_{T,p,m^{\text{S}},m^{\text{A}},m^{\text{WV}}}\frac{\mathrm{d}m^{\text{V}}}{\mathrm{d}t} = L^{\text{SA}}J_m. \quad (37)$$

688 This expression of energy conservation, the 1$^{\text{st}}$ law of thermodynamics, is similarly valid for
689 equilibrium and non-equilibrium conditions of the sample. For comparison, of the total entropy
690 defined by,

691 $$N^{\text{SA}} \equiv m^{\text{SW}}\eta^{\text{SW}} + m^{\text{AV}}\eta^{\text{AV}}, \quad (38)$$

692 the change is given by

693 $$\frac{dN^{SA}}{dt} = \left(\frac{\partial N^{SA}}{\partial m^V}\right)_{T,p,m^S,m^A,m^{WV}} \frac{dm^V}{dt}.$$ (39)

694 In terms of its two parts, eq. (38), this change takes the form,

695 $$\frac{dN^{SA}}{dt} = \left[\eta^{AV} - A\left(\frac{\partial \eta^{AV}}{\partial A}\right)_{T,p} - \eta^{SW} + S\left(\frac{\partial \eta^{SW}}{\partial S}\right)_{T,p}\right] J_m.$$ (40)

696 In oceanography, the symbol N for entropy was suggested by Fofonoff (1962) to avoid confusion
697 with salinity S. Making use of their local equilibria, specific entropy of each part can be expressed by
698 the difference, eq. (B.6),

699 $$\eta = \frac{h-g}{T},$$ (41)

700 between specific enthalpy, h, and specific Gibbs energy, g, so that the entropy change (40) becomes

701 $$T\frac{dN^{SA}}{dt} = \left(L^{SA} + \Delta\mu\right)J_m.$$ (42)

702 Here, the latent heat, L^{SA}, is given by eq. (23), and the distance from mutual equilibrium, $\Delta\mu$, by eq.
703 (24).

704 The first term,

705 $$T\frac{d_e N^{SA}}{dt} \equiv L^{SA} J_m,$$ (43)

706 is the *external* entropy change (subscript e) in the form of the heat flux required to maintain the
707 sample's temperature, in the sense of Maxwell's (1888) definition of latent heat, compensating the
708 storage of latent heat by emitting water vapour.

709 The second term,

710 $$T\frac{d_i N^{SA}}{dt} \equiv J_m \Delta\mu.$$ (44)

711 is the *internal* entropy change (subscript i), or *entropy production*, of the non-equilibrium sea-air
712 sample. It represents the additional entropy gain of humid air compared to the entropy loss of
713 seawater. This production happens at the air-sea interface and disappears as soon as mutual
714 equilibrium, $\Delta\mu = 0$, is approached.

715 It is important to be aware that the external part, $\frac{d_e N^{SA}}{dt}$, *always* constitutes a contribution to the
716 system's energy balance while, by contrast, the internal part, $\frac{d_i N^{SA}}{dt}$, is *never* any such contribution.
717 The irreversible production of entropy is an internal conversion or redistribution of energy rather
718 than a change of it. This implies that irreversible processes violate Gibbs' fundamental equation (B.8)
719 in the sense that

720 $$\frac{dH^{SA}}{dt} = -T\frac{d_e N^{SA}}{dt} + V^{SA}\frac{dp}{dt} + \sum_i \mu_i \frac{dm_i}{dt} > -T\frac{dN^{SA}}{dt} + V^{SA}\frac{dp}{dt} + \sum_i \mu_i \frac{dm_i}{dt},$$ (45)

721 even though each of its local-equilibrium elements strictly satisfies the related fundamental equation
722 (B.13), valid for reversible processes only,

723 $$dh = -Td\eta + vdp + \sum_{i=1}^{n-1}(\mu_i - \mu_0)dw_i.$$ (46)

724 Entropy production appears wherever a flux is passing its driving gradient. Near equilibrium, this flux
725 is proportional to its driving force (Glansdorff and Prigogine 1971, Landau and Lifschitz 1974, Kraus

726 and Businger 1994, Feistel and Hellmuth 2024a), usually termed *Onsager force*. For example, the
727 evaporation mass flux of water, eq. (6),

728 $$J_m = C \, \Delta\mu \qquad\qquad (47)$$

729 may be assumed as being proportional to the difference between the chemical potentials of water
730 across the air-sea interface. The related *Dalton equation* (6) was discussed in Section 4. The
731 associated entropy production, eq. (44), obeys the 2nd law of thermodynamics by the inequality

732 $$\frac{\mathrm{d_i} N^{SA}}{\mathrm{d}t} = C \, (\Delta\mu)^2 \geq 0, \qquad\qquad (48)$$

733 while the total entropy change, eq. (42) may possess any sign. In other words, the 2nd law forbids that
734 *Onsager fluxes* may be directed against their causing Onsager forces. The *Prigogine Theorem* predicts
735 that in linear irreversible thermodynamics, entropy production approaches minimum values at
736 steady states (Glansdorff and Prigogine 1971).

737 Processes accompanied by entropy production are termed *irreversible* ones, since entropy once
738 created may never be destroyed again. Related processes cannot be reversed unless lasting changes
739 are left behind in the external world. By contrast, processes which transform an equilibrium state
740 into another equilibrium state may *reversibly* be performed without producing entropy. Entropy
741 production is possible only under non-equilibrium conditions.

742 Under typical marine circumstances, the entropy production density of ocean evaporation can be
743 estimated to about 4 mW K^{-1} m^{-2}, contributing roughly 0.4 % to the global entropy production
744 (Feistel and Ebeling 2011, Feistel and Hellmuth 2024a).

745

746

747 **6   Cloudiness and Ocean Warming**

748 "Cloud feedback on climate represents the largest uncertainty in our ability to understand the
749 sensitivity of the planet to radiative forcing" (Gettelman and Sherwood 2016). On the long-term
750 average, cloudiness is particularly strong in the low-pressure belts of the global tropospheric
751 circulation, where air is ascending and its humidity is condensing, see Fig. 12. Except for the
752 equatorial zone, those spatial cloudiness pattern correlate visibly with those of recent ocean
753 warming, compare Fig. 1. It is a plausible working hypothesis that this correlation could also indicate
754 a causal relation between the two phenomena. However, such correlations imply chicken-and-egg
755 problems (Rapp 2014): putative causality relations between those trends cannot be derived from
756 observation but only be concluded from reliable prediction models (Feistel 2023). May the observed
757 systematic reduction of global cloudiness (Fasullo and Trenberth 2012) actually be responsible for
758 the currently recorded excessive ocean warming (You 2024)? Unfortunately, and somewhat
759 surprisingly, this assumption can apparently not be underpinned yet by closer investigation. Some
760 related issues will be discussed in this section.
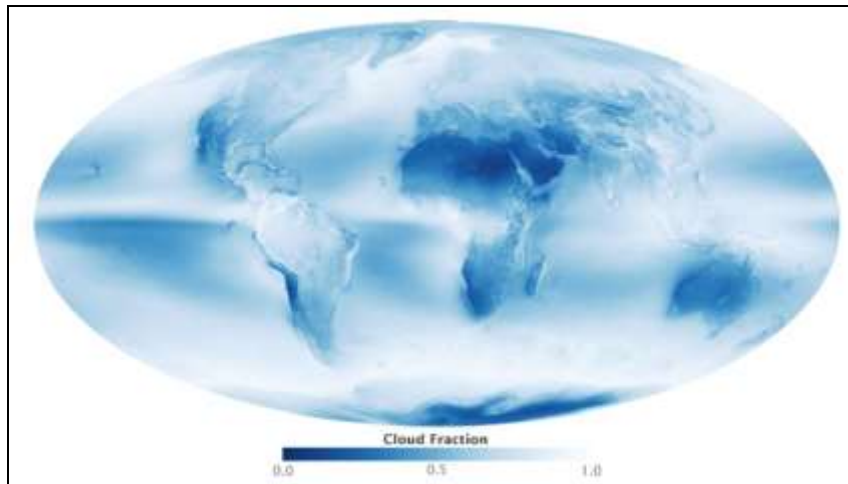
Fig. 12: Global distribution of cloudiness July 2002 – April 2015 (Allen and Ward 2015). Image reproduction permitted by NASA Copyright.

6.1 Cloudiness Trend

Global cloud-covered surface area fraction C has systematically been reducing by about 6 % per century, see Fig. 13, from $C \approx 67.5$ % in 1980 to $C \approx 65$ % in 2022 (Foster et al. 2023, Phillips and Foster 2023). Observed cloudiness values depend strongly on the way clouds are defined (Spänkuch et al. 2022) and on the measurement technology applied. For example, Rapp (2014: Fig. 6.20) reported a decrease in cloudiness in 30 years from 70 % in 1983 down to 63.5 % in, likely, 2013. This reduction rate of more than 20 % per century is three times as fast as that given in Fig. 13 and may result from different observation techniques.

Assuming that this shrinking occurred in a similar way above both land and sea, the ocean is expected to receive increasingly more solar irradiation. This phenomenon is known as the *short-wave cloud radiative effect* (SW CRE), see Fig. 14.

On the other hand, clouds are opaque with respect to oceanic upward thermal radiation and emit themselves downward infrared radiation. This phenomenon is known as the *long-wave cloud radiative effect* (LW CRE), see Fig. 15. Radiation models show that on the global average these two effects cancel each other almost completely up to minor residual of -1 mW m^{-2} yr^{-1}, so that the continuously shrinking cloudiness may be assumed to have practically no net effect on the ocean's radiation balance (Phillips and Foster 2023, Feistel and Hellmuth 2024b). However, more detailed investigations in the future may reveal more rigorous results for the ocean than this simplified picture.
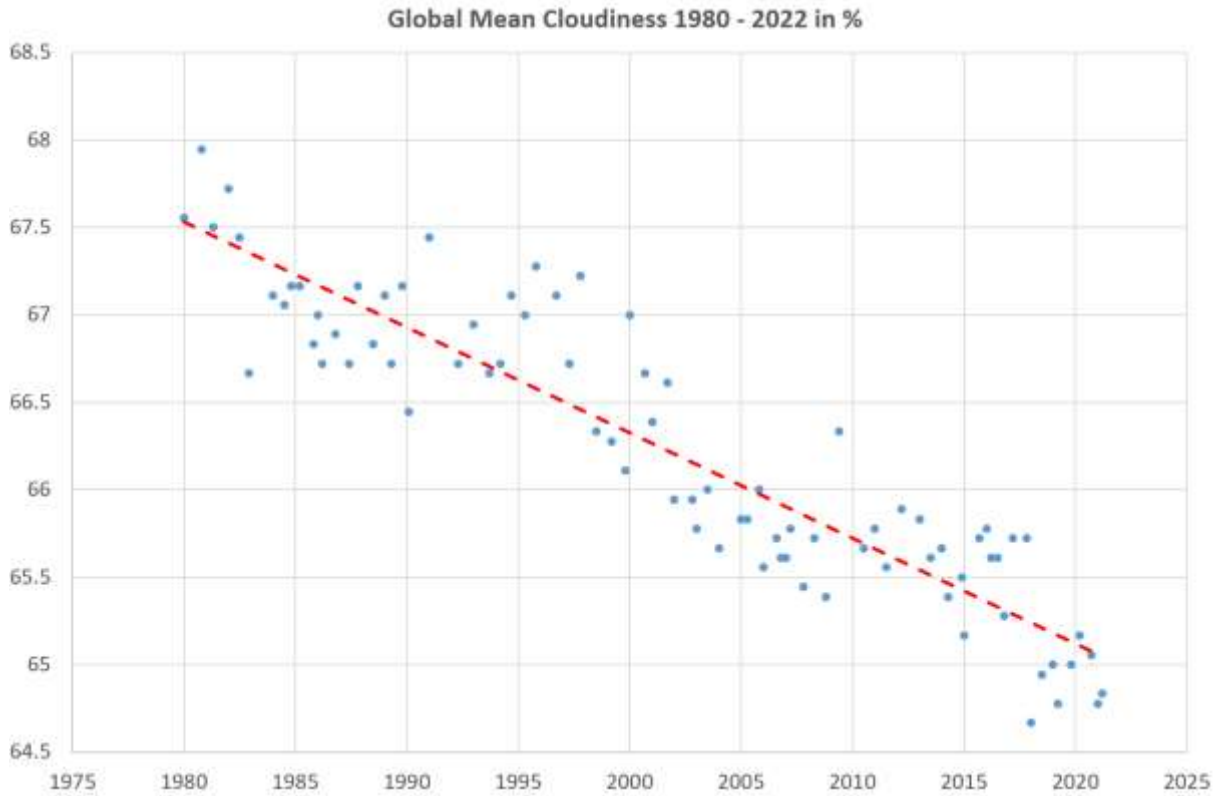
Fig. 13: Dots: satellite-derived global mean cloud area fractions 1980-2022 in percent. Data from
Foster et al. (2023). Dashed line: present cloudiness is 65 % with a climatological linear shrinking
trend of −6.2 % per century.
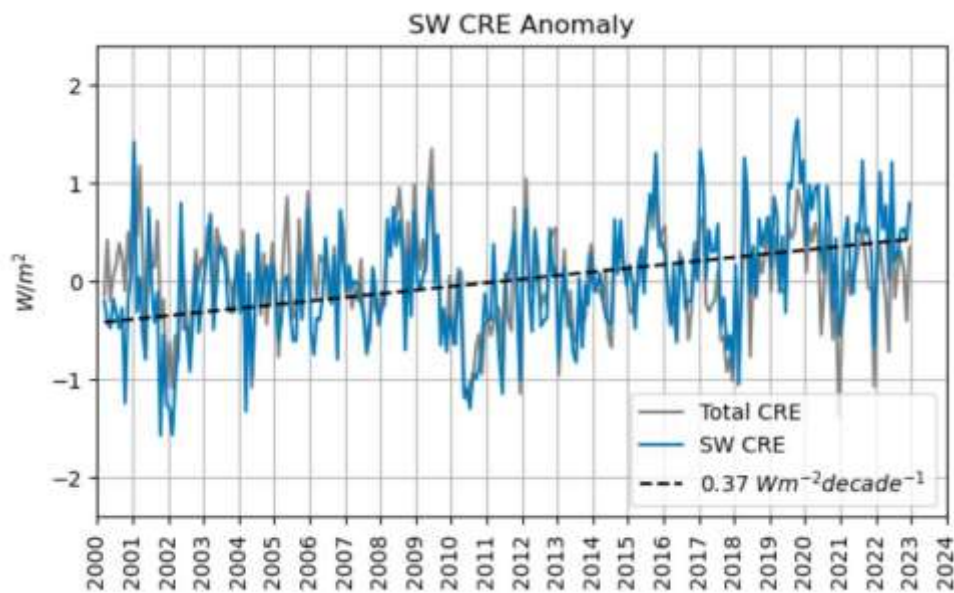
Fig. 14: Short-wave cloud radiative effect (SW CRE) of increasing solar irradiation. Image kindly
provided by Coda Phillips (priv. comm.), with minor correction compared to the similar previous
publication (Phillips and Foster 2023). Total CRE is the net effect of SW and LW CRE, see Fig. 15
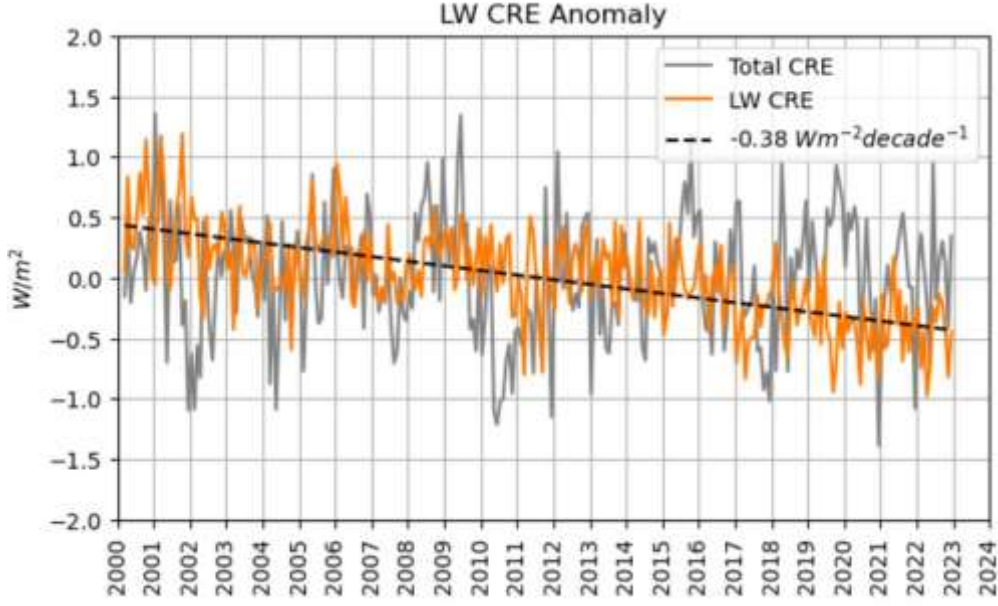
792

793 Fig. 15: Long-wave cloud radiative effect (LW CRE) of decreasing net thermal radiation. Image kindly
794 provided by Coda Phillips (priv. comm.), with minor correction compared to the similar previous
795 publication (Phillips and Foster 2023). Total CRE is the net effect of SW and LW CRE, see Fig. 14.

796

797 *6.2 Cumulus Clouds*

798 Cumulus clouds are often formed in the course of diurnal convection by isentropic uplift of humid air
799 parcels from the sea surface to the condensation level, mostly located at low heights between 200
800 and 500 m. This process permits a thermodynamic description of such clouds (Romps 2014) by
801 calculating the *lifted condensation level* (LCL) as the cumulus cloud base. In distinction to previous
802 studies, as the first such international geophysical standard, TEOS-10 provides explicit equations for
803 entropy, enthalpy and chemical potentials of humid air which may be used to derive reference
804 equations and values of the LCL (Feistel and Hellmuth 2024b).

805 At the sea surface pressure, p_{SS}, the air parcel may possess the temperature T_{SS} and the relative
806 fugacity ψ_f, which is a real-gas definition of relative humidity (Feistel and Lovell-Smith 2017) in terms
807 of the chemical potential of water vapour in humid air, μ_V^{AV}, and that of liquid water, μ_W,

808 $$R_W T_{SS} \ln \psi_f = \mu_V^{AV}(A, T_{SS}, p_{SS}) - \mu_W(T_{SS}, p_{SS}).$$ (49)

809 Here, $R_W = 461.523 \text{ J kg}^{-1} \text{ K}^{-1}$ is the specific gas constant of water, and $A = 1 - q$ is the dry-air
810 mass fraction of the parcel, to be determined from ψ_f by this condition.

811 At the LCL, the parcel is saturated at $\psi_f = 1$, i.e.,

812 $$0 = \mu_V^{AV}(A, T_{LCL}, p_{LCL}) - \mu_W(T_{LCL}, p_{LCL}).$$ (50)

813 During uplift, A is assumed to remain constant, as well as the parcel's entropy, η^{AV},

814 $$\eta^{AV}(A, T_{SS}, p_{SS}) = \eta^{AV}(A, T_{LCL}, p_{LCL}).$$ (51)

815
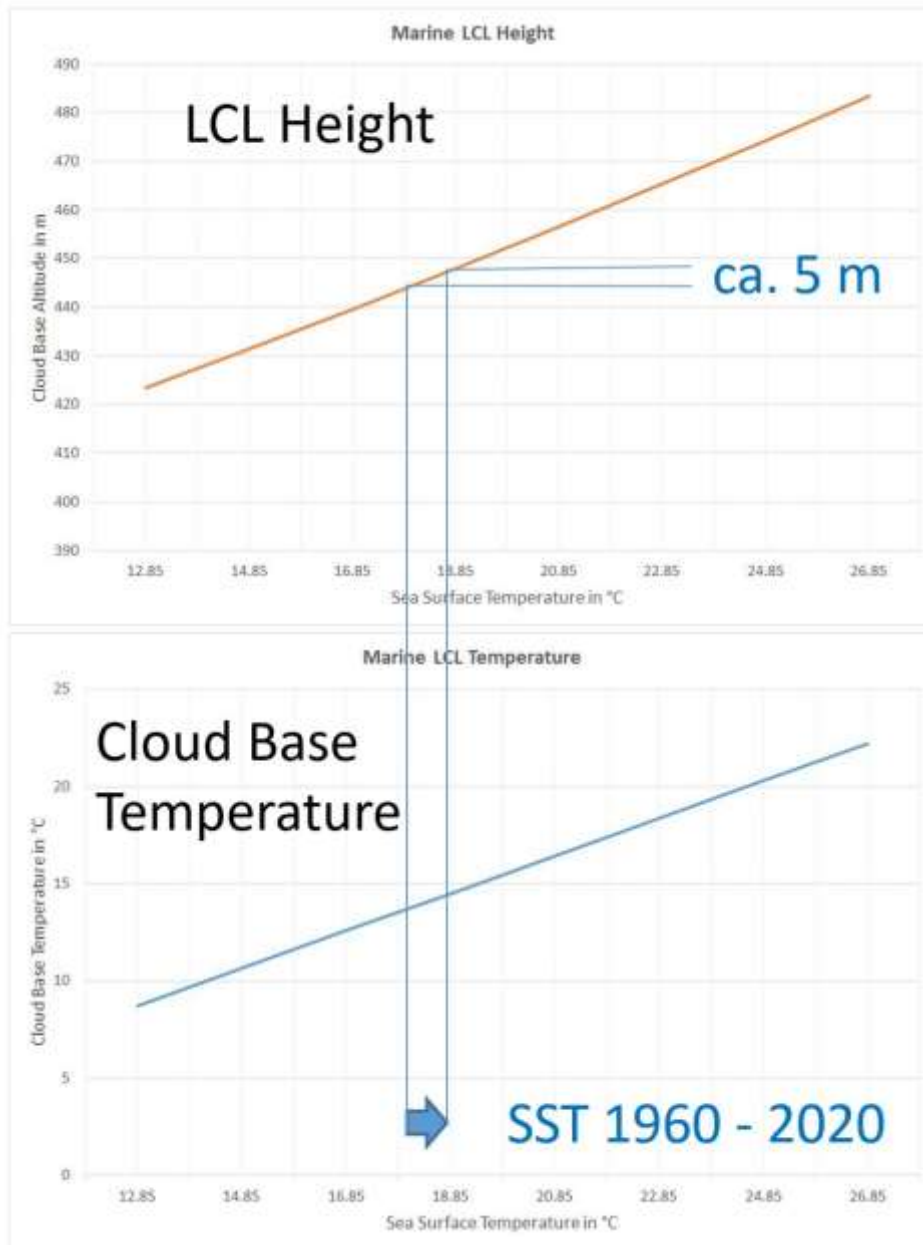
816

817 Fig. 16: As a function of typical low-latitude sea-surface temperatures, LCL height (top) and LCL
818 temperature (bottom) are computed from the TEOS-10 equations (49) – (52) at a typical marine
819 surface RH of 80 %rh. The added interval indicates the global mean SST change between 1960 and
820 2020 which has resulted in an increase of the cloud base altitude by about 5 m.

821

822

823
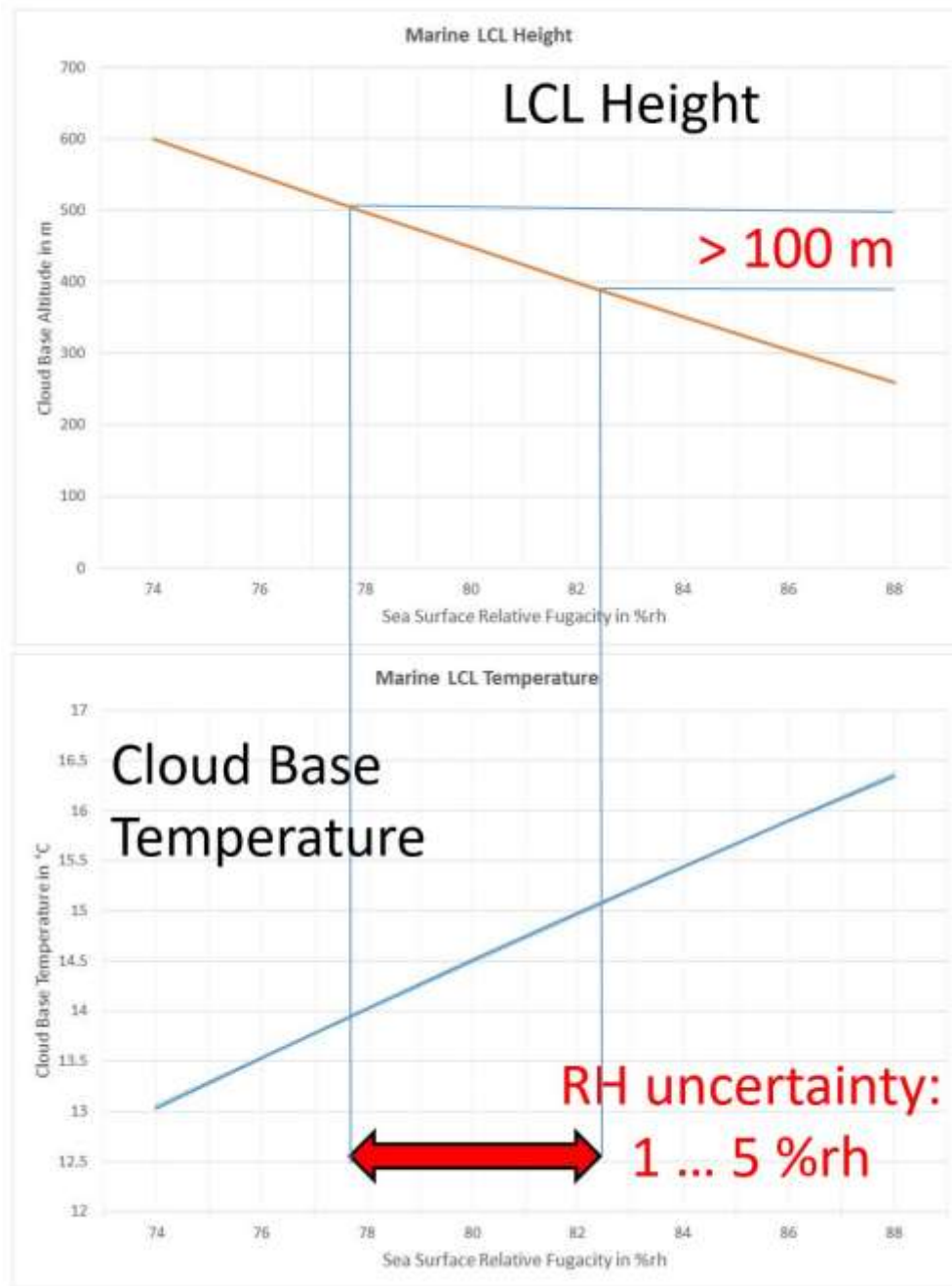
Fig. 17: As a function of typical marine RH values, LCL height (top) and LCL temperature (bottom) are computed from the TEOS-10 equations (49) – (52) at a sea surface temperature of 292 K, close to the current global mean SST of 18.8 °C, see Fig. 18. The added interval indicates the observation uncertainty of sea surface RH which corresponds to an uncertainty of the cloud base altitude of more than 100 m.

829

Finally, the LCL altitude, z_{LCL}, above sea level follows from the isentropic integral of the hydrostatic equation in terms of the enthalpy, h^{AV}, of humid air,

$$z_{\mathrm{LCL}} = \frac{1}{g_{\mathrm{E}}} \left[h^{\mathrm{AV}}\left(A, \eta^{\mathrm{AV}}, p_{\mathrm{SS}}\right) - h^{\mathrm{AV}}\left(A, \eta^{\mathrm{AV}}, p_{\mathrm{LCL}}\right) \right]. \tag{52}$$

The gravity acceleration is $g_{\mathrm{E}} = 9.81 \ \mathrm{m \ s^{-2}}$. The functions $\mu_{\mathrm{V}}^{\mathrm{AV}}$, η^{AV}, h^{AV} and μ_{W} can be expressed by partial derivatives of the TEOS-10 thermodynamic potentials of humid air and liquid water, and

835 are numerically available from the *Sea-Ice-Air* (SIA) *library* (Feistel et al. 2010d, Wright et al. 2010).

836 Solving eqs. (49) – (52) numerically, the LCL properties $(A, T_{\text{LCL}}, p_{\text{LCL}}, z_{\text{LCL}})$ are obtained from the

837 given surface properties, $(\psi_f, T_{\text{SS}}, p_{\text{SS}})$.

838 Table 1: LCL cloud-base temperatures, T_{LCL}, pressures, p_{LCL}, and heights, z_{LCL}, as functions of the

839 SST, T_{SS}, at marine surface relative fugacity of $\psi_f = 80$ %rh, computed from TEOS-10 eqs. (49) –

840 (52), as well as climatic LCL sensitivities, α, β, γ, eq. (53), with respect to increasing SST (Feistel and

841 Hellmuth 2024). The row printed in bold approximates the current global mean SST, see Fig. 18.

T_{SS} K	T_{LCL} K	p_{LCL} hPa	z_{LCL} m	α % K^{-1}	β K K^{-1}	γ hPa K^{-1}
286	281.883	963.093	423.468	−0.0483	0.9634	−0.2742
288	283.810	962.542	431.481	−0.0542	0.9629	−0.2773
290	285.735	961.984	439.660	−0.0608	0.9624	−0.2806
292	**287.659**	**961.419**	**448.017**	**−0.0680**	**0.9619**	**−0.2841**
294	289.583	960.847	456.561	−0.0759	0.9614	−0.2878
296	291.505	960.268	465.305	−0.0846	0.9608	−0.2917
298	293.426	959.680	474.263	−0.0942	0.9603	−0.2959
300	295.346	959.084	483.449	−0.1047	0.9597	−0.3004

842

843
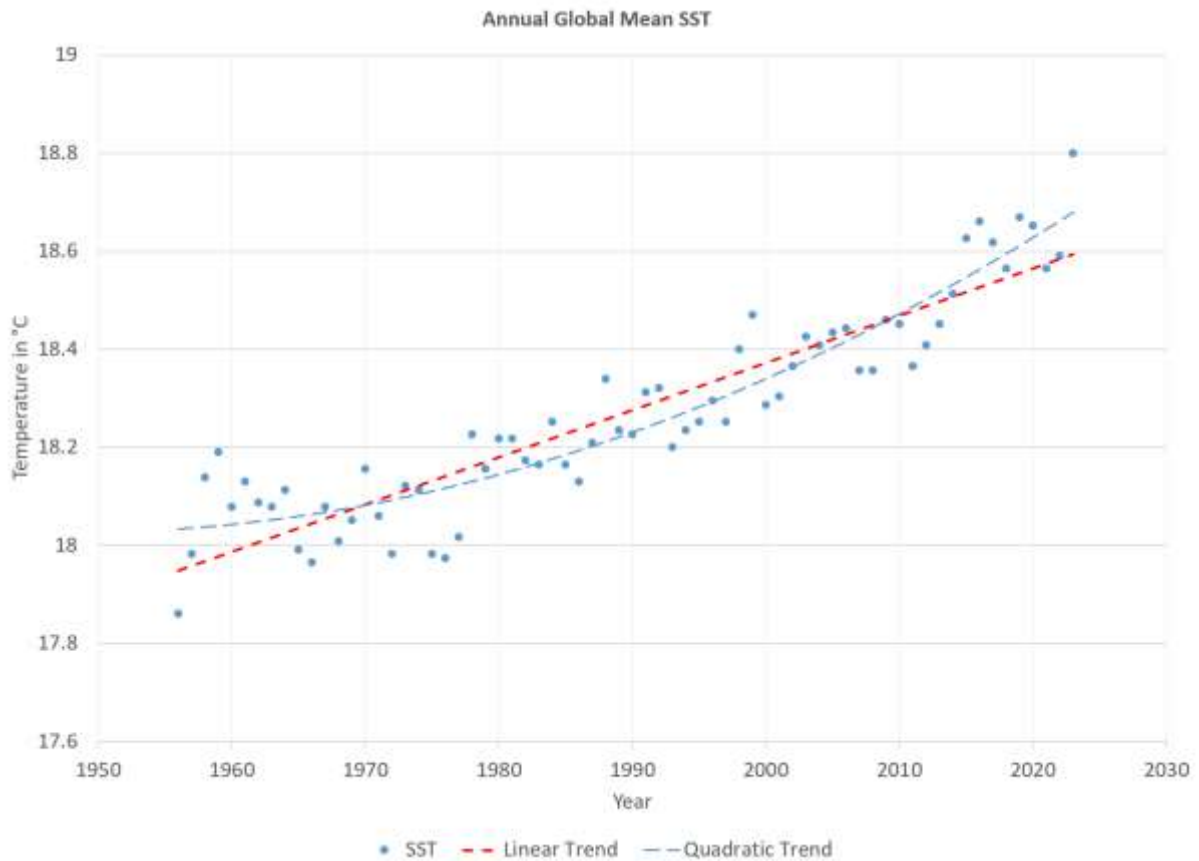
844

845 Fig. 18: Estimated increase 1957 – 2023 of global annual mean sea-surface temperatures (source:

846 Cheng et al. 2024). The linear trend (red) is $t/°C \approx 18 + 0.01 \times (yr - 1961)$. The quadratic trend

847 curve (blue) suggests an acceleration of warming.

848

849 As solutions of eqs. (49) – (52), height and base temperature of marine cumulus clouds, as a function
850 of the sea-surface temperature T_0 at a sea-surface relative fugacity of $\psi_f = 80$ %rh, are displayed in
851 Fig. 16. Similarly, height and base temperature, as a function of the sea-surface relative fugacity RF of
852 ψ_f at a sea-surface temperature $T_{SS} = 292$ K, close to the current global mean SST, are displayed in
853 Fig. 17. It is obvious that the LCL effect of the range of RF uncertainty exceeds significantly the effect
854 caused by global SST rise, so that unknown minor systematic RF changes may easily disguise the
855 thermal effects on marine cumulus clouds.

856 Global mean sea-surface temperature has risen from about 17.9 °C in 1956 to 18.8 °C in 2023 (Cheng
857 et al. 2024), see Fig. 18. This pronounced climatic trend is expected to let the cumulus cloud base lift
858 up while at the same time warming it, see Fig. 16, but not as much as the SST itself is increasing. The
859 related climatic sensitivities possess complicated dependencies but may directly be derived by taking
860 the related derivatives

861 $$\alpha \equiv \left(\frac{\partial A}{\partial T_{SS}}\right)_{p_{SS},\psi_f} = -\left(\frac{\partial q}{\partial T_{SS}}\right)_{p_{SS},\psi_f}, \beta \equiv \left(\frac{\partial T_{LCL}}{\partial T_{SS}}\right)_{p_{SS},\psi_f} \text{ and } \gamma \equiv \left(\frac{\partial p_{LCL}}{\partial T_{SS}}\right)_{p_{SS},\psi_f}, \qquad (53)$$

862 of the TEOS-10 LCL equations (49) – (52) with respect to the surface temperature while keeping
863 surface RH fixed (Feistel and Hellmuth 2024). Selected results for those sensitivities are given in Table
864 1 relative to 1 °C rise of SST, similar to that in the past 70 years (Fig. 16). Here, $\alpha \approx -0.07$ % K^{-1}
865 describes the rate of increase of specific humidity at the sea surface, often dubbed the "Clausius-
866 Clapeyron effect". The value of $\beta \approx 0.96$ indicates that the cumulus cloud base warms up slower
867 that the ocean by about 4 %, and $\gamma \approx -0.28$ hPa K^{-1} is the LCL pressure lowering caused by ocean
868 warming, corresponding to ascending clouds. The value $\beta < 1$ implies that the thermal downward
869 radiation from the cloud base does not keep pace with the ocean upward radiation, so that the net
870 climatic feedback of cumulus clouds is negative and acts against ocean warming. These clouds do not
871 provide a physical explanation for the observed enhanced ocean warming.

872

873 *6.3 Stratocumulus and Other Clouds*

874 "Marine low clouds strongly cool the planet" (Myers et al. 2021). Over the Atlantic, "the strongest
875 surface longwave cloud effects were shown in the presence of low level clouds" (Kalisch and Macke
876 2012). "Low-cloud feedbacks are also a leading cause of uncertainty in future climate prediction
877 because even small changes in cloud coverage and thickness have a major impact on the radiation
878 budget" (Wood 2012: p. 2373).

879 Generally, however, the dominating cloud type over the ocean is stratocumulus (Eastman et al.
880 2011). "They are common over the cooler regions of subtropical and midlatitude oceans where their
881 coverage can exceed 50% in the annual mean" (Wood 2012: p. 2373) with a typical thickness about
882 320 m and "a tendency for thicker clouds (median 420 m) in mid- and high latitudes" (Wood 2012: p.
883 2378). "Stratocumuli tend to form under statically stable lower-tropospheric conditions" (Wood
884 2012: p. 2374). On the annual average, stratocumulus is particularly frequent (up to 60 % coverage)
885 at the subtropical coastal upwelling regions such as the cold Benguela, Humboldt and California
886 Currents (Wood 2012: Fig. 4a, Muhlbauer et al. 2014: Fig. 2). However, in those areas there is no
887 obvious correlation of cloud cover with ocean warming (Fig. 1). Stratocumulus also forms large cloud
888 cover (about 20 % coverage) in the boreal and austral west-wind bands (Wood 2012: Fig. 4a) where
889 the ocean is strongly warming up (Fig. 1).

890 "Only small changes in the coverage and thickness of stratocumulus clouds are required to produce a
891 radiative effect comparable to those associated with increasing greenhouse gases" (Wood 2012: p.

892   2374). Marine stratocumulus cloud feedback is still a major challenge and source of uncertainty of
893   climate models (Hirota et al. 2021). However, "similar to other low-cloud types in the marine
894   boundary layer, the impact of stratocumulus clouds on the outgoing longwave radiation is marginal
895   due to the lack of contrast between the temperature of stratocumulus cloud tops and the
896   temperature of the sea surface over which they form. Thus, the net radiative effect of stratocumulus
897   clouds is primarily controlled by factors influencing their shortwave cloud forcing such as the cloud
898   albedo and the cloud coverage" (Muhlbauer et al. 2014: p. 6695).

899   Following this argumentation and assuming that the short-wave cloud effect of stratocumuli on the
900   ocean radiation balance by far outweighs their long-wave effects, then the short-wave warming
901   effect (Fig. 14) of decreasing cloudiness may dominate over the long-wave cooling (Fig. 15). Possibly,
902   this could make stratocumulus a potential candidate for causing the unclear recent ocean warming.

903   Similarly, in the diurnal cycle, short-wave effects (Fig. 14) have an impact at daytime only, while long-
904   wave effects (Fig. 15) are present all 24 hours. In this respect, Luo et al. (2024) report that low-level
905   cloudiness has an asymmetric day/night trend which enhances ocean warming. Regionally, where in
906   spring the days get longer, and the heavy cloudiness of the west-wind belt becomes replaced by
907   fewer subtropical clouds (see Fig. 12), the systematic reduction of cloudiness may be expected to
908   produce local excess warming such as near the subtropical fronts (see Fig. 1). Only dedicated future
909   model studies, however, may reliably verify such speculations. As a recent example for the
910   complexity of SST warming "by suppressing the evaporative cooling" of the ocean, Wang et al. (2024)
911   explain dramatic but yet elusive warming events in the North-East Pacific by changes in ocean-
912   atmosphere mechanisms caused by reduced Chinese aerosol emissions. Also, Berthou et al. (2024)
913   describe cloud cover feedback over the sea during an unprecedented marine heatwave off northwest
914   Europe in 2023.

915

916   7   Summary

917   Substantial uncertainties of estimated heat fluxes at the ocean-atmosphere interface, such as the
918   "ocean heat budget closure problem", prevent reliable model predictions and causal explanations of
919   climate phenomena that may take place within the range of those uncertainties. Among such
920   "surprises" is the currently registered excessive ocean warming, but are also the subsequent
921   consequences of this warming, such as those expected for global weather processes.

922   Intending to reduce model uncertainties of thermal energies and heat fluxes in the climate system
923   associated with the global circulation of water in its different phases and mixtures, the new
924   geophysical thermodynamic standard TEOS-10 had been adopted internationally in 2009 and 2011.
925   Meanwhile, the uptake of TEOS-10 by the scientific community is mainly focussed on ocean
926   observations and modelling, as the related publication metrics are suggesting (Appendix A).

927   TEOS-10 is advanced over previous similar standards and various collections of tailored empirical
928   property equations by (i) its completeness in describing all thermodynamic properties of seawater,
929   humid air and ice, including their entropies, enthalpies and chemical potentials, by (ii) its perfect
930   mutual consistency between different phases and mixtures, and by (iii) its minimum uncertainty over
931   maximum ranges of validity. Among its particularly favourable fields of application are composite
932   systems with internal phase boundaries such as air sea interaction or cloud formation.

933   In addition to entropies, enthalpies and chemical potentials, TEOS-10 has made available certain new
934   quantities for the description and modelling of climate processes, such as (i) Absolute Salinity of the
935   ocean with a specified Reference Composition, (ii) Conservative Temperature as a measure of

936 Potential Enthalpy of seawater representing a definite heat content, and (iii) Relative Fugacity as the
937 thermodynamic driving force of evaporation, suggesting an improved full-range definition of relative
938 humidity as a substitute for mutually inconsistent and restricted such definitions in practical use in
939 climatology, meteorology and physical chemistry.

940 This paper explains some tutorial examples for the application of TEOS-10 to selected current climate
941 problems. There is (i) the two-phase conceptual model of "sea air" which provides rigorous equations
942 for the latent heat of evaporation, for the heat capacity of humid air including salty aerosols (sea
943 spray), and for the irreversible production of entropy by evaporation into the marine troposphere.
944 There is also (ii) the formation of low marine cumulus clouds by isentropic thermal convection up to
945 their condensation level, and their climatic feedback to surface temperature and humidity
946 concerning their infrared radiation effects.

947 It is currently unclear why and how the ocean warming is intensifying, and when and how the related
948 enormous amount of heat may transfer to the atmosphere. The observed systematic reduction of
949 cloudiness may play an important role in this process, but responsible details and theoretical causes
950 are unknown. Marine surface relative humidity is an important and rather sensitive "control valve"
951 for the supply of the troposphere with latent heat, however, the common assumption of constant
952 relative humidity during climate change lacks rigorous explanation and leaves open the question of
953 its possible trends below the insufficiently high level of observational uncertainty. TEOS-10 may
954 further assist climate modellers to address such issues.

955 Ocean Science has proved a scientifically well-reputable, reliable and successful partner journal for
956 the publication of advanced results and methods in oceanography and geophysics. Cooperation with
957 international bodies such as IUGG, UNESCO/IOC, IAPSO, SCOR, IAPWS and BIPM has made possible
958 the development and international introduction of TEOS-10. The established standing committee JCS
959 remains active with respect to related fundamental problems yet to be solved. It is hoped and
960 expected that TEOS-10 may constitute a reliable long-term thermodynamic basis for interdisciplinary
961 climate research.

962

963 **Appendix A: Summary and Metrics of Selected Publications Related to TEOS-10**

964 Between December 2008 and December 2012, supporting the activities of SCOR/IAPSO WG127,
965 *Ocean Science* had published 16 articles open-access in its Special Issue #14, "Thermophysical
966 properties of seawater" (Feistel et al. 2008a). From February 2013 on, monthly metrics have been
967 recorded by the journal. Table A1 reports those metrics of the last decade.

968 For comparison, metrics – as far as published elsewhere by 04 April 2024 – of selected TEOS-10
969 articles listed at www.teos-10.org are reported in Table A2.

970 **Table A1**: Metrics of articles in the *Ocean Science* Special Issue #14, "Thermophysical properties of
971 seawater" (Feistel et al. 2008a), from February 2013 till March 2024. "SIA" stands for the TEOS-10
972 Sea-Ice-Air open source code library.

Reference	Topic	Accessed	PDF Downloads	Cited
Millero and Huang (2009)	Seawater at High T,S	16 462	11 061	79
Feistel et al. (2010c)	Baltic Sea Density/Salinity	15 435	11 385	92
Pawlowicz et al. (2011)	Seawater Biogeochemistry	9 663	6 444	47
McDougall et al. (2012)	Global Absolute Salinity	9 290	5 489	116
Feistel et al. (2010a)	Humid Air Helmholtz Function	8 737	5 346	31

Safarov et al. (2009)	Seawater at High T,p	7 356	4 308	68
Wright et al. (2011)	Density Salinity	5 268	2 891	49
Marion et al. (2009)	CaCO$_3$ Solubility	5 169	3 170	36
Pawlowicz (2010)	Composition Variation	4 471	2 666	27
Feistel et al. (2010d)	SIA Library Equations	4 255	2 416	23
Wright et al. (2010)	SIA Library Routines	4 049	1 733	19
Feistel et al. (2008b)	Consistent New Potentials	3 585	1 527	27
Seitz et al. (2011)	Salinity Traceability	3 363	1 705	24
Feistel et al. (2010b)	Baltic Property Anomalies	3 183	1 500	12
Tailleux (2009)	Mixing Efficiency	2 752	1 303	11
Millero and Huang (2010)	Seawater at High T,S (corrig.)	2 189	909	1

973

974 **Table A2**: Metrics published by March 2024 of selected TEOS-10 related articles apart from *Ocean*
975 *Science* Special Issue #14. "Ice Ih" is the ambient, hexagonal ice I phase of water.

Reference	Topic	Accessed	PDF Downloads	Cited
Wagner and Pruß (2002)	Water Helmholtz Function	7 516	7 516	3 457
Jackett et al. (2006)	Algorithms for Seawater	2 877	2 364	119
Feistel (2005)	Seawater Gibbs Function	2 584	1 126	10
Feistel et al. (2005)	Ice Ih Gibbs Function	2 288	1 015	5
Lemmon et al. (2000)	Dry Air Helmholtz Function	2 279	2 279	381
McDougall (2003)	Potential Enthalpy	1 970	1 367	50
Wagner et al. (2011)	Ice Melting/Sublimation	1 467	510	102
Seitz et al. (2010)	Salinity Determination	1 332		15
Feistel (2008b)	IAPWS-06 and IAPWS-08	1 279		4
Millero et al. (2008)	Seawater Composition	970		780
Feistel and Wagner (2006)	Ice Ih Gibbs Function	843	843	286
Feistel and Wagner (2005)	Ice Ih Gibbs Function	833		58
Graham and McDougall (2013)	Conservative Temperature	651	467	28
Feistel (2012)	New TEOS-10 Standard	436		27
Spall et al. (2013)	TEOS-10 for oceanography	230	128	3
Feistel (2008a)	Seawater Gibbs Function	134		133
Roquet et al. (2015)	TEOS-10 Polynomials	111		97
Feistel and Wagner (2007)	Ice Ih Sublimation >20 K	105		112
Feistel (2003)	Seawater Gibbs Function	100		105
McDougall et al. (2013)	Thermodynamics of Seawater	35		10
Feistel and Marion (2007)	Seawater Gibbs-Pitzer	25		32
Valladares et al. (2011)	Replacement of EOS-80	14+5		4+1
Feistel et al. (2006)	New Seawater Equation			

976

977 **Table A3**: IAPWS documents supporting TEOS-10, openly accessible at www.iapws.org. IAPWS
978 documents are independently and painstakingly verified before they may become adopted at an
979 annual meeting. No metrics available.

Document	Code	Topic	Meeting	Year
Release	R06-95	Water Helmholtz Function	Dresden	2016
Release	R10-06	Ice Ih Gibbs Function	Doorwerth	2009
Release	R13-08	Seawater Gibbs Function	Berlin	2008
Release	R14-08	Ice Melting/Sublimation	Pilsen	2011

Suppl. Release	SR1-86	Water Saturation Properties	St. Petersburg	1992
Suppl. Release	SR6-08	Liquid Water at 0.1 MPa	Pilsen	2011
Suppl. Release	SR7-09	Liquid Water Gibbs Function	Doorwerth	2009
Guideline	G05-01	Fundamental Constants	Virtual Online	2020
Guideline	G08-10	Humid Air Helmholtz Function	Niagara Falls	2010
Guideline	G09-12	Cold Water Vapour < 130 K	Boulder	2012
Guideline	G11-15	Fugacity Virial Equation	Stockholm	2015
Guideline	G12-15	Supercooled Water	Stockholm	2015
Advisory Note	AN4-09	IAPWS/CIPM Water Density	Doorwerth	2009
Advisory Note	AN5-13	Industrial Seawater	Dresden	2016
Advisory Note	AN6-16	IAPWS support for TEOS-10	Dresden	2016

980

981 **Table A4:** Numbers of unique internet downloads 2011-2023 of supporting material from the TEOS-
982 10 homepage at www.teos-10.org. "GSW" stands for the TEOS-10 Gibbs Seawater open source code
983 library. Data from Pawlowicz (2023)

Item	2011-13	2013-14	2014-15	2015-16	2016-17	2017-18	2018-19	2019-20	2020-21	2021-22	2022-23
TEOS-10 Manual	920	360	535	552	418	427	349	472	479	482	530
Getting Started	879	362	558	547	427	475	349	444	460	483	479
Lecture Slides	704	284	374	318	219	248	204	272	272	231	272
TEOS-10 Primer	584	197	289	297	222	217	187	253	260	226	268
GSW MATLAB	1920	1102	1485	1814	1235	1552	1233	1556	1504	1747	1897
GSW FORTRAN	366	222	171	162	127	116	82	98	83	92	87
GSW C	202	84	133	151	85	96	59	81	58	49	57
GSW PHP	-	55	61	43	29	60	28	52	22	22	21
SIA VB	72	100	46	45	45	48	43	47	47	38	30
SIA FORTRAN	59	118	58	44	36	42	37	42	31	33	31

984

985 **Table A5**: Selected additional TEOS-10 related readings, metrics by March 2024

Reference	Topic	Accessed	PDF Downloads	Cited
Turner et al. (2016)	Seawater Pitzer Model	13 780	1 175	21
Lovell-Smith et al. (2016)	Relative Humidity Challenges		6 502	27
Schmidt et al. (2018)	Density-Salinity Relation	9 421	5 481	28
Feistel et al. (2016a)	Challenges beyond TEOS-10		5 023	49
Dickson et al. (2016)	Seawater pH Challenges		2 818	43
Pawlowicz et al. (2016)	Seawater Salinity Challenges		2 738	40
Smythe-Wright et al. (2019)	IAPSO's history and roles	5 893	384	3
Foken et al. (2021)	Atmospheric Measurements	5 709		2
Feistel (2018)	TEOS-10 Review	5 441	1 632	38
Feistel and Hellmuth (2023)	Dalton Equation	5 068		1

McDougall et al. (2021)	Ocean Heat Flux and Content	4 993	1 425	5
Hellmuth et al. (2020)	Ice-Crystal Nucleation	4 811		6
Uchida et al. (2019)	Optical Density Sensor	3 513		19
Hellmuth et al. (2021)	Mass Density of Humid Air	2 643		4
Feistel and Lovell-Smith (2017)	Relative Fugacity Part 1		1 335	18
Le Menn et al. (2018)	Seawater Salinity Measurands		1 136	13
Schmidt et al. (2016)	Seawater Density up to 1 ppm		950	21
Ji et al. (2021)	Absolute Salinity off China	2 462	856	3
Von Rohden et al (2016)	Baltic Sound Speed	2 122	784	1
Feistel et al. (2016b)	Uncertainty of Correlation Eqs.		662	14
Martins and Cross (2022)	TEOS-10 Excel Code	2 087	542	2
Hellmuth and Feistel (2020)	Low-Density Subcooled Water	1 827		1
Feistel (2011a)	Stochastic Potential Functions	1 217		6
McDougall et al. (2014)	Sea Ice Formation	1 124	771	16
Feistel and Hellmuth (2024a)	Evaporation Entropy	1 038		0
Young (2010)	Boussinesq Approximation	928	724	56
Harvey et al. (2023)	Water Properties	874	369	9
Tailleux (2018)	Local Available Potential Energy	807	409	11
Uchida et al. (2020)	Seawater Intercomparison	707	764	6
Sharkawy et al. (2010)	Review of Seawater Correlations	701		946
Feistel (2019a)	Relative Fugacity Part 2		267	3
Feistel et al. (2022)	Relative Fugacity Part 3		252	4
McDougall et al. (2023)	Seawater Potential of (S, CT, p)	629	122	1
Feistel et al. (2015)	Virial Fugacity Equation	581		17
Nayar et al. (2016)	Seawater Property Review	553		366
Marion et al. (2011)	Seawater pH	491		170
Feistel and Lovell-Smith (2023)	Systematic Error in Regression	428	41	
Holzapfel and Klotz (2024)	H_2O and D_2O Ice Ih	285	58	
Ji et al. (2024)	Bohai Sea Salinity Anomaly	254	56	
Holzapfel and Klotz (2021)	Thermal Expansion of Ice Ih	245	77	1
Pawlowicz and Feistel (2012)	TEOS-10 in Limnology			22
Kretzschmar et al. (2015)	Industrial Seawater Equation	104		0
Ebeling et al. (2020)	Individual Ionic Activities	99		10
Marion et al. (2010)	FREZCHEM Solution Model	82		74
Sun et al. (2008)	Saline Thermal Fluid Equations	79		84
Almeida et al. (2018)	TEOS-10 Atlantic Impact	53		5
Safarov et al. (2012)	High-Salinity Seawater	42		21
Woosley et al. (2014)	World Ocean Absolute Salinity	39		16
Safarov et al. (2013)	Brackish Seawater Properties	35		15
Ulfsbo et al. (2015)	Seawater Activity Coefficients	34		11
Feistel and Hagen (1998)	Sea Ice Gibbs Function	24		31
Feistel (2010)	Seawater Gibbs Function	23		24
Tailleux (2010)	Buoyancy Power Input			20
Millero and Huang (2011)	Seawater Compressibility	19		19
Tchijov et al. (2008)	Ice at High p and Low T	19		6
Von Rohden et al. (2015)	Seawater Sound Speed 0.1 MPa			18
Budéus (2018)	TEOS-10 Density Bias ?	8		5
Lago et al. (2015)	Seawater Sound Speed < 70 MPa	8		4
Manaure et al. (2021)	Individual Ionic Activities	8		2
Weinreben and Feistel (2019)	Anomalous Salinity Density	8		1
Pawlowicz & Yerubandi (2024)	Water as a Substance	4		0

Ebeling et al. (2022)	Individual Ionic Activities	2		6
Waldmann et al. (2022)	Uncertainty of Ocean Variables	2		
Tailleux and Dubos (2024)	Seawater Static Energy	1		1
Pawlowicz (2013):	Physical Variables in the Ocean			
Laliberte (2015)	TEOS-10 Python Code			
Thol et al. (2024)	N_2-O_2-Ar Helmholtz Function			

986

987 **Appendix B: Thermodynamic Potentials**

988 This Appendix provides a short introduction to thermodynamic potentials, supporting the equations
989 and topics discussed in this article. Alternative presentations from different perspectives are
990 available from numerous textbooks such as Guggenheim (1949), Margenau and Murphy (1964),
991 Landau and Lifschitz (1966) or Kittel (1969). For seawater, the use of a Gibbs thermodynamic
992 potential was first suggested theoretically by Fofonoff (1958, 1962), see also Craig (1960).

993 A key theoretical tool for the physical investigation of the globally warming climate and the related
994 energy balances is *thermodynamics*. It is known from experience that there exists a distinguished
995 state of various ambient substances that is known as a *thermodynamic equilibrium state*. If a sample
996 of matter is in this state, it may never spontaneously alter its measurable macroscopic properties
997 unless it becomes disturbed by external contact and exchange of energy or matter with its
998 surrounding. Typical properties which characterise a particular equilibrium state are the total mass of
999 a sample, *m*, its volume, *V*, its temperature, *T*, or its pressure, *p*. Of a given sample, different
1000 equilibrium states may exist that differ in those quantities, but there exists a specific relation
1001 between those variables, known as an *equation of state*, which is characteristic for the given
1002 substance and remains universally valid at any of its possible equilibrium states. The most general
1003 and comprehensive equation of state of a given substance is a *thermodynamic potential* of that
1004 substance.

1005 Thermodynamics is a mathematical theory for the construction and exploitation of equations of state
1006 and of properties derived therefrom for the prediction or verification of observations or experiments.
1007 Depending on the properties of interest, equations of state may be formulated in various different
1008 mathematical forms. It was discovered by J. Willard Gibbs (1873) that from a suitable thermodynamic
1009 potential all thermodynamic properties of a given substance at any of its equilibrium states can be
1010 derived by appropriate mathematical methods.

1011 For theoretical reasons (namely, the statistical so-called *canonical ensemble*, Landau and Lifschitz
1012 1966: §31; Kittel 1969: Ch. 18), a preferred thermodynamic potential of a pure substance is its
1013 *Helmholtz Energy*, or *Free Energy*, $F(m, T, V)$, expressed in terms of the sample's mass, m, its
1014 temperature und volume. For mixtures, the single mass must be replaced by the set of partial masses
1015 of the species involved. Here, mass is used as a measure for the amount of substance, rather than
1016 particle or mole numbers, for the practical reason that in oceanography masses are easier measured
1017 than moles, and so TEOS-10 is following that tradition and is a mass-based description. Classical
1018 empirical thermodynamics of Clausius and Gibbs was formulated independently of the existence and
1019 properties of atoms or molecules which presently define the mole (BIPM 2019).

1020 To the *Internal Energy E* of the sample, the Helmholtz energy is related by the Helmholtz Differential
1021 Equation,

1022 $$E = F - T \left(\frac{\partial F}{\partial T}\right)_{m,V} \qquad (B.1)$$

1023 Note that IOC et al. (2010) uses the symbol U for the Internal Energy rather than E in eq. (B.1). This
1024 replacement is done here for denoting with u the wind speed, eq. (6), rather than specific internal
1025 energy, which is defined here by $e = E/m$, eqs. (1) and (B.3). The symbol E is frequently used in the
1026 thermodynamic literature, for example by Gibbs (1873a) and Landau and Lifschitz (1966).

1027 The potential function F is extensive, which means that for instance $F(2\,m, T, 2\,V) = 2\,F(m, T, V)$ is
1028 valid for an equilibrium sample of twice the mass. It follows that the mass-specific Helmholtz
1029 function, $F/m \equiv f(T, \rho)$, depends on two variables only, T and the mass density, $\rho \equiv m/V$, and is
1030 mathematically simpler and more convenient than F, which may always be retrieved from a given f
1031 by

1032 $$F(m, T, V) = m \times f\left(T, \frac{m}{V}\right). \tag{B.2}$$

1033 The quantitative description of a substance of interest in the form of a thermodynamic potential such
1034 as $f(T, \rho)$ has axiomatic properties. The description is *complete*, i.e., all thermodynamic properties of
1035 that substance are available, it is *consistent*, i.e., for any property one and only one result can be
1036 derived, and it is *independent*, i.e., no part of this description may be omitted without loosing the
1037 completeness. It is obvious that such axiomatic properties are very desirable for the description of
1038 geophysical substances, however, such thermodynamic potentials are rarely found in the
1039 corresponding literature. In particular in climate research which combines results and data from
1040 different disciplines, such as meteorology and oceanography, from research carried out all over the
1041 globe and over the years by subsequent generations of specialists, international binding standards
1042 such as the International System of Units (SI) are required that ensure mutual consistency and
1043 metrological comparability of any involved data produced from experiments, observations and
1044 models.

1045 Gibbs' (1873a) original potential function was (internal) energy, $e = E/m$. It is known that a sample's
1046 energy can be increased by compression, $-p\,dv$, where $v = 1/\rho$ is the specific volume, or by input of
1047 heat, $T\,d\eta$, where $\eta = N/m$ is the specific entropy. As an extensive quantity, entropy introduced by
1048 Clausius (1865, 1976) is denoted here by N to avoid confusion with seawater salinity, S. Energy
1049 conservation implies that

1050 $$de = T\,d\eta - p\,dv. \tag{B.3}$$

1051 Any such change between different equilibrium states of the same sample takes place along a
1052 definite, substance-specific surface $e(\eta, v)$ so that de in eq. (B.3) is mathematically an exact
1053 differential and the partial derivatives of e possess the physical meanings that

1054 $$T = \left(\frac{\partial e}{\partial \eta}\right)_v, \qquad -p = \left(\frac{\partial e}{\partial v}\right)_\eta. \tag{B.4}$$

1055 Gibbs (1873b) also demonstrated that for several equilibrium samples in contact with one another, in
1056 absence of gravity or accelerated motion, the samples are in mutual equilibrium only if they have
1057 equal values of the coefficients T and p of eq. (2.3).

1058 In the geophysical practice, the quantities η and v are difficult to measure, in contrast to, say, T or p.
1059 Mathematically equivalent to $e(\eta, v)$, thermodynamic potentials in terms of the other three possible
1060 pairs of independent variables are formally obtained from so-called Legendre transforms (Alberty
1061 2001), namely the *Helmholtz function* $f(T, v) \equiv e - T\eta$ with the differential

1062 $$df = -\eta\,dT - p\,dv, \tag{B.5}$$

1063 the *Gibbs function* $g(T, p) \equiv f + pv = e - T\eta + pv$ with

1064 $\mathrm{d}g = -\eta \mathrm{d}T + v\mathrm{d}p,$ (B.6)

1065   and the specific *enthalpy* $h(\eta, p) \equiv g + T\eta = f + T\eta + pv = e + pv$ with

1066 $\mathrm{d}h = T\mathrm{d}\eta + v\mathrm{d}p.$ (B.7)

1067   Depending on the application purpose, each of these potential functions has certain advantages and
1068   disadvantages, and having all of them optionally at hand in mutually consistent versions is most
1069   useful.

1070   Gibbs (1874-78) also considered a situation in which a given sample may exchange substance with its
1071   surrounding. If the exchanged mass of substance *i* is $\mathrm{d}m_i$, the related change of the sample's
1072   (extensive) energy E at constant entropy and volume is termed the *chemical potential* μ_i of that
1073   substance,

1074 $\mathrm{d}E = T\mathrm{d}N - p\mathrm{d}V + \sum_i \mu_i\, \mathrm{d}m_i,$ (B.8)

1075   so that this exact differential implies that the chemical potential is obtained from

1076 $\mu_i \equiv \left(\frac{\partial E}{\partial m_i}\right)_{N,V,m_{j\neq i}} = \left(\frac{\partial F}{\partial m_i}\right)_{T,V,m_{j\neq i}} = \left(\frac{\partial G}{\partial m_i}\right)_{T,p,m_{j\neq i}} = \left(\frac{\partial H}{\partial m_i}\right)_{N,p,m_{j\neq i}}.$ (B.9)

1077   Equilibrium of a spatially extended substance, in absence of gravity or accelerated motion, requires
1078   that in addition to T and p, also the chemical potential μ_i separately for each present substance
1079   needs to possess the same value anywhere in the volume. "The potential for each component
1080   substance must be constant throughout the whole mass" (Gibbs 1874-78: p. 119).

1081   As intensive properties, the specific energies cannot depend on the total mass but only on the mass
1082   fractions, $w_i \equiv m_i/m$. Because by definition $\sum w_i = 1$, only $(n-1)$ different fractions may be
1083   independent variables describing the n components of a mixture. For example, one of the
1084   components may be chosen as a master species, "0", such as a solvent, and the remaining ones, $i = $
1085 $1, \ldots, n-1$, may denote the solutes.

1086   In terms of T and p, chemical potentials are computed from the Gibbs function, g, through the Gibbs
1087   energy, G, of eq. (B.9). Because the Gibbs function depends only on the independent intensive
1088   variables, $g(w_1, \ldots, w_{n-1}, T, p)$, the solutes' chemical potentials, $i > 0$, are

1089 $\mu_i = \left(\frac{\partial G}{\partial m_i}\right)_{T,p,m_{j\neq i}} = \left(\frac{\partial(m\,g)}{\partial m_i}\right)_{T,p,m_{j\neq i}} = g + \left(\frac{\partial g}{\partial w_i}\right)_{T,p,w_{j\neq i}} - \sum_{j=1}^{n-1} w_j \left(\frac{\partial g}{\partial w_j}\right)_{T,p,w_{k\neq j}}$ (B.10)

1090   Similarly, the solvent's chemical potential is

1091 $\mu_0 = \left(\frac{\partial G}{\partial m_0}\right)_{T,p,m_{j>0}} = \left(\frac{\partial(m\,g)}{\partial m_0}\right)_{T,p,m_{j>0}} = g - \sum_{j=1}^{n-1} w_j \left(\frac{\partial g}{\partial w_j}\right)_{T,p,w_{k\neq j}}.$ (B.11)

1092   Therefore, the *relative chemical potentials* of the solutes are simply the partial derivatives,

1093 $\mu_i - \mu_0 = \left(\frac{\partial g}{\partial w_i}\right)_{T,p,w_{j\neq i}}.$ (B.12)

1094   For mixtures, $n > 1$, the differential (B.6) of the Gibbs function takes the more general form

1095 $\mathrm{d}g = -\eta \mathrm{d}T + v\mathrm{d}p + \sum_{i=1}^{n-1}(\mu_i - \mu_0)\mathrm{d}w_i.$ (B.13)

1096   It follows straightforwardly from (B.10), (B.11) that the sum,

1097 $\sum_{i=0}^{n-1} \mu_i\, m_i = m\,g = G,$ (B.14)

1098   equals the Gibbs energy itself (Gibbs 1874-78: eq. (96) therein, Guggenheim 1949, Landau and

1099   Lifschitz 1966, Kittel 1969). In particular, if $n = 1$, the Gibbs function g of a pure substance

1100   represents its chemical potential,

1101 $g = \mu.$ (B.15)

1102   Where two phases of a pure substance are in contact at mutual equilibrium, such as saturated water

1103   vapour at the liquid water surface, the mathematically distinct Gibbs functions of those phases take

1104   equal values. This indispensable condition for mutual consistency between the thermodynamic

1105   potentials of TEOS-10 is rigorously obeyed by virtue of appropriate reference-state conditions (Feistel

1106   et al. 2008b).

1107   *Code/Data availability*. TEOS-10 library code used for this paper is available from www.teos-10.org

1108   *Competing interests*. The author has declared that he has no competing interests.

1109   *Acknowledgements.* The author is grateful to Karen Heywood for her kind invitation to write this

1110   Ocean Science Jubilee article. This paper contributes to the tasks of the International Joint

1111   SCOR/IAPWS/IAPSO Committee on the Properties of Seawater (JCS) and was presented at the 18th

1112   International Conference on the Properties of Water and Steam (ICPWS) at Boulder, Co. (Feistel

1113   2024).

1114

1115   **References**

1116   Abraham, J.P., Baringer, M., Bindoff, N.L., Boyer, S.T., Cheng, L.J., Church, J.A., Conroy, J.L.,

1117   Domingues, C.M., Fasullo, J.T., Gilson, J., Goni, G., Good, S.A., Gorman, J.M., Gouretski, V., Ishii, M.,

1118   Johnson, G.C., Kizu, S., Lyman, J.M., Macdonald, A.M., Minkowycz, W.J., Moffitt, S.E., Palmer, M.D.,

1119   Piola, A.R., Reseghetti, F., Schuckmann, K., Trenberth, K.E., Velicogna, I., and Willis, J.K.: A Review of

1120   Global Ocean Temperature Observations: Implications for Ocean Heat Content Estimates and Climate

1121   Change, Reviews of Geophysics 51, 450-483, https://doi.org/10.1002/rog.20022, 2013.

1122   Alberty, R.A.: Use of Legendre transforms in chemical thermodynamics, Pure Appl. Chem. 73, 1349–

1123   1380, https://doi.org/10.1351/pac200173081349, 2001.

1124   Albrecht, F.: Untersuchungen über den Wärmehaushalt der Erdoberfläche in verschiedenen

1125   Klimagebieten, Reichsamt für Wetterdienst, Wissenschaftliche Abhandlungen Bd. VIII, Nr. 2, Springer,

1126   Berlin, Heidelberg, https://doi.org/10.1007/978-3-662-42530-5, 1940.

1127   Allen, J. and Ward, K.: Cloudy Earth. NASA Earth Observatory image using data provided by the

1128   MODIS Atmosphere Science Team, NASA Goddard Space Flight Center,

1129   https://earthobservatory.nasa.gov/images/85843/cloudy-earth, 2015.

1130   Almeida, L., Lima de Azevedo, J.L., Kerr, R., Araujo, M., and Mata, M.M.: Impact of the new equation

1131   of state of seawater (TEOS-10) on the estimates of water mass mixture and meridional transport in

1132   the Atlantic Ocean, Progress in Oceanography 162, 13-24,

1133   https://doi.org/10.1016/j.pocean.2018.02.008, 2018.

1134   Azorin-Molina, C., Dunn, R.J.H., Ricciardulli, L., Mears, C.A., Nicolas, J.P., McVicar, T.R., Zeng, Z., and

1135   Bosilovich, M.G.: Land and Ocean Surface Winds, in: Blunden, J., Boyer, T., Bartow-Gillies, E. (eds.):

1136   State of the Climate in 2022, Bull. Amer. Meteor. Soc. 104, S72–S74, https://doi.org/10.1175/BAMS-

1137   D-23-0090.1, 2023.

Baumgartner, A. and Reichel, E.: The World Water Balance, R. Oldenbourg Verlag, München, Germany, 1975.

Berthou, S.,Renshaw, R., Smyth, T., Tinker, J., Grist, J.P., Wihsgott, J.U., Jones, S., Inall, M., Nolan, G., Berx, B., Arnold, A., Blunn, L.P., Castillo, J.M., Cotterill, D., Daly, E., Dow, G., Gómez, B., Fraser-Leonhardt, V., Hirschi, J.J.-M., Lewis, H.W., Mahmood, S., and Worsfold, M.: Exceptional atmospheric conditions in June 2023 generated a northwest European marine heatwave which contributed to breaking land temperature records, Communications Earth & Environment 5, 287, https://doi.org/10.1038/s43247-024-01413-8, 2024.

BIPM: The International System of Units (SI), Bureau International des Poids et Mesures, Sèvres, https://www.bipm.org/en/publications/si-brochure , 2019.

Biswas, A.K.: Experiments on Atmospheric Evaporation until the End of the Eighteenth Century. Technology and Culture 10, 49-58, https://doi.org/10.2307/3102003, 1969.

Budéus, G. Th.: Potential bias in TEOS10 density of sea water samples, Deep-Sea Res. Pt. I, 134, 41–47, https://doi.org/10.1016/j.dsr.2018.02.005, 2018.

Budyko, M.I.: Der Wärmehaushalt der Erdoberfläche, Fachliche Mitteilungen der Inspektion Geophysicalischer Beratungsdienst der Bundeswehr im Luftwaffenamt, Köln, Germany, Vol. 100, pp. 3–282, 1963.

Budyko, M.I.: Evolyutsiya Biosfery, Gidrometeoizdat, Leningrad, 1984.

Cahill, B.E., Kowalczuk, P., Kritten, L., Gräwe, U., Wilkin, J., and Fischer, J.: Estimating the seasonal impact of optically significant water constituents on surface heating rates in the western Baltic Sea, Biogeosciences 20, 2743–2768, https://doi.org/10.5194/bg-20-2743-2023, 2023.

Carlon, H.R.: Infrared emission by fine water aerosols and fogs, Appl. Opt. 9, 2000-2006, https://doi.org/10.1364/AO.9.002000, 1970.

Carlon, H.R.: Aerosol spectrometry in the infrared, Appl. Opt. 19, 2210-2218, https://doi.org/10.1364/AO.19.002210, 1980.

Cheng, L., Abraham, J., Trenberth, K.E., Boyer, T., Mann, M.E., Zhu, J., Wang, F., Yu, F., Locarnini, R., Fasullo, J., Zheng, F., Li, Y., Zhang, B., Wan, L., Chen, X., Wang, D., Feng, L., Song, X., Liu, Y., Reseghetti, F., Simoncelli, S., Gouretski, V., Chen, G., Mishonov, A., Reagan, J., Von Schuckmann, K., Pan, Y., Tan, Z., Zhu, Y., Wei, W., Li, G., Ren, Q., Cao, L., and Lu, Y.: New record ocean temperatures and related climate indicators in 2023, Advances in Atmospheric Sciences, https://doi.org/10.1007/s00376-024-3378-5, 2024.

Clausius, R.: Ueber verschiedene für die Anwendung bequeme Formen der Hauptgleichungen der mechanischen Wärmetheorie, Annalen der Physik 201, 353–400, https://doi.org/10.1002/andp.18652010702, 1865.

Clausius, R.: Die Mechanische Wärmetheorie, Friedrich Vieweg, Braunschweig, 1876.

Craig, H.: The Thermodynamics of Sea Water, Proc. Nat. Acad. Sci. 46, 1221-1225, https://doi.org/10.1073/pnas.46.9.1221, 1960.

Dai, A.: Recent Climatology, Variability, and Trends in Global Surface Humidity, J. Clim. 19, 3589–3606, https://doi.org/10.1175/JCLI3816.1, 2006.

1177   Debski, K.: Continental Hydrology, Volume 2: Physics of Water, Atmospheric Precipitation, and
1178   Evaporation, Scientific Publications Foreign Cooperation Center of the Central Institute, Warsaw,
1179   1966.

1180   Dickson, A.G., Camões, M.F., Spitzer, P., Fisicaro, P., Stoica, D., Pawlowicz, R., and Feistel, R.:
1181   Metrological challenges for measurements of key climatological observables, Part 3: Seawater pH,
1182   Metrologia 53, R26–R39, https://doi.org/10.1088/0026-1394/53/1/R26 , 2016.

1183   Eastman, R., Warren, S.G., and Hahn, C.J.: Variations in Cloud Cover and Cloud Types over the Ocean
1184   from Surface Observations, 1954–2008, J. Climate 24, 5914-5934,
1185   https://doi.org/10.1175/2011JCLI3972.1, 2011.

1186   Ebeling, W. and Feistel, R.: Physik der Selbstorganisation und Evolution. Akademie-Verlag, Berlin,
1187   1982.

1188   Ebeling, W., Feistel, R., and Camoes, M.F.: Trends in statistical calculations of individual ionic activity
1189   coefficients of aqueous electrolytes and seawater, Trends in Physical Chemistry 20, 1-26,
1190   http://www.researchtrends.net/tia/abstract.asp?in=0&vn=20&tid=16&aid=6609&pub=2020&type=3
1191   , 2020.

1192   Ebeling, W., Feistel, R., and Krienke, H.: Statistical theory of individual ionic activity coefficients of
1193   electrolytes with multiple-charged ions including seawater, Journal of Molecular Liquids 346, 117814,
1194   https://doi.org/10.1016/j.molliq.2021.117814, 2022.

1195   Emden, R.: Über Strahlungsgleichgewicht und atmosphärische Strahlung, Sitzungsber. Akad. Wiss.
1196   München 1, 55-142, https://www.zobodat.at/pdf/Sitz-Ber-Akad-Muenchen-math-Kl_1913_0001.pdf ,
1197   1913.

1198   Falkenhagen, H., Ebeling, W., and Hertz, H.G.: Theorie der Elektrolyte, S. Hirzel Verlag, Leipzig, 1971.

1199   Fasullo, J.T. and Trenberth, K.E.: A Less Cloudy Future: The Role of Subtropical Subsidence in Climate
1200   Sensitivity, Science 338, 792-794, https://doi.org/10.1126/science.1227465, 2012.

1201   Feistel, R.: Thermodynamics of Seawater, in: Striggow, K. Schröder, A. (eds.): German Democratic
1202   Republic National Report for the period 1.1.1987–2.10.1990 (Final Report) IAPSO, presented at the
1203   XX. General Assembly of the IUGG, Wien 1991, Institut für Meereskunde, Warnemünde,
1204   https://doi.org/10.13140/RG.2.1.3973.3282, 1991.

1205   Feistel, R.: Equilibrium thermodynamics of seawater revisited, Prog. Oceanogr. 31, 101–179,
1206   https://doi.org/10.1016/0079-6611(93)90024-8, 1993.

1207   Feistel, R.: A new extended Gibbs thermodynamic potential of seawater, Progress in Oceanography
1208   58, 43-114, https://doi.org/10.1016/S0079-6611(03)00088-0, 2003.

1209   Feistel, R.: Numerical implementation and oceanographic application of the Gibbs thermodynamic
1210   potential of seawater, Ocean Sci., 1, 9–16, https://doi.org/10.5194/os-1-9-2005, 2005.

1211   Feistel, R.: A Gibbs function for seawater thermodynamics for −6 to 80°C and salinity up to 120 g kg^{-1},
1212   Deep Sea Research Part I 55, 1639-1671, https://doi.org/10.1016/j.dsr.2008.07.004, 2008a.

1213   Feistel, R.: Thermodynamics of water, vapor, ice, and seawater, Accred. Qual. Assur. 13, 593–599,
1214   https://doi.org/10.1007/s00769-008-0443-1, 2008b.

1215   Feistel, R.: Extended equation of state for seawater at elevated temperature and salinity,
1216   Desalination 250, 14–18, https://doi.org/10.1016/j.desal.2009.03.020, 2010.

1217   Feistel, R.: Stochastic ensembles of thermodynamic potentials, Accred. Qual. Assur. 16, 225–235,
1218   https://doi.org/10.1007/s00769-010-0695-4, 2011a.

1219   Feistel, R.: Radiative entropy balance and vertical stability of a gray atmosphere, Eur. Phys. J. B 82,
1220   197–206, https://doi.org/10.1140/epjb/e2011-20328-2, 2011b.

1221   Feistel, R.: TEOS-10: A New International Oceanographic Standard for Seawater, Ice, Fluid Water, and
1222   Humid Air, Int. J. Thermophys. 33, 1335–1351, https://doi.org/10.1007/s10765-010-0901-y, 2012.

1223   Feistel, R.: Salinity and relative humidity: Climatological relevance and metrological needs, Acta
1224   Imeko 4, 57–61, http://dx.doi.org/10.21014/acta_imeko.v4i4.216, 2015.

1225   Feistel, R.: Thermodynamic properties of seawater, ice and humid air: TEOS-10, before and beyond,
1226   Ocean Sci. 14, 471–502, https://doi.org/10.5194/os-14-471-2018, 2018.

1227   Feistel, R.: Defining relative humidity in terms of water activity. Part 2: relations to osmotic pressures,
1228   Metrologia 56, 015015. https://doi.org/10.1088/1681-7575/aaf446, 2019a

1229   Feistel, R.: Distinguishing between Clausius, Boltzmann and Pauling Entropies of Frozen Non-
1230   Equilibrium States, Entropy 21, 799, https://doi.org/10.3390/e21080799, 2019b.

1231   Feistel, R.: On the Evolution of Symbols and Prediction Models, Biosemiotics 16, 311–371,
1232   https://doi.org/10.1007/s12304-023-09528-9, 2023.

1233   Feistel, R.: Thermodynamics of Water in the "Steam Engine" Climate, IAPWS Gibbs Award Lecture, 24
1234   June 2024, 18th International Conference on the Properties of Water and Steam, Boulder, Colorado,
1235   USA, https://doi.org/10.13140/RG.2.2.15038.50248/1, 2024.

1236   Feistel, R. and Ebeling, W.: Physics of Self-Organization and Evolution, Wiley-VCH, Weinheim, 2011.

1237   Feistel, R. and Hagen, E.: On the GIBBS thermodynamic potential of seawater, Prog. Oceanogr. 36,
1238   249–327, https://doi.org/10.1016/S0165-232X(98)00014-7, 1995.

1239   Feistel, R. and Hagen, E.: A Gibbs thermodynamic potential of sea ice, Cold Regions Science and
1240   Technology 28, 83–142, https://doi.org/10.1016/S0165-232X(98)00014-7, 1998.

1241   Feistel, R. and Hellmuth, O.: Relative Humidity: A Control Valve of the Steam Engine Climate, J. Hum.
1242   Earth Future 2, 140–182, https://doi.org/10. 28991/HEF-2021-02-02-06, 2021.

1243   Feistel, R. and Hellmuth, O.: Thermodynamics of Evaporation from the Ocean Surface, Atmosphere
1244   14, 560, https://doi.org/10.3390/atmos14030560, 2023.

1245   Feistel, R. and Hellmuth, O.: Irreversible Thermodynamics of Seawater Evaporation, J. Mar. Sci. Eng.
1246   12, 166, https://doi.org/10.3390/jmse12010166, 2024a.

1247   Feistel, R. and Hellmuth, O.: TEOS-10 Equations for Determining the Lifted Condensation Level (LCL)
1248   and Climatic Feedback of Marine Clouds, Oceans 2024, 5(2), 312-351.
1249   https://doi.org/10.3390/oceans5020020, 2024b.

1250   Feistel, R., Hellmuth, O. and Lovell-Smith, J.: Defining relative humidity in terms of water activity. III:
1251   Relations to dew-point and frost-point temperatures, Metrologia 59, 045013,
1252   https://doi.org/10.1088/1681-7575/ac7185, 2022.

1253   Feistel, R. and Lovell-Smith, J.W.: Defining relative humidity in terms of water activity. Part 1:
1254   definition, Metrologia 54, 566–576, https://doi.org/10.1088/1681-7575/aa7083, 2017.

1255 Feistel, R. and Lovell-Smith, J.W.: Uncertainty Propagation using Dispersion Matrices Accounting for
1256 Systematic Error in Least-Squares Regression, Preprints 2023, 2023111917,
1257 https://doi.org/10.20944/preprints202311.1917.v1, 2023.

1258 Feistel, R., Lovell-Smith, J.W., and Hellmuth, O.: Virial Approximation of the TEOS-10 Equation for the
1259 Fugacity of Water in Humid Air, Int. J. Thermophys. 36, 44–68, https://doi.org/10.1007/s10765-014-
1260 1784-0, 2015.

1261 Feistel, R., Lovell-Smith, J.W., Saunders, P., and Seitz, S.: Uncertainty of empirical correlation
1262 equations, Metrologia 53, 1079, https://doi.org/10.1088/0026-1394/53/4/1079, 2016.

1263 Feistel, R. and Marion, G.M.: A Gibbs–Pitzer function for high-salinity seawater thermodynamics,
1264 Prog. Oceanogr. 74, 515–539, https://doi.org/10.1016/j.pocean.2007.04.020, 2007.

1265 Feistel, R., Marion, G.M., Pawlowicz, R., and Wright, D.G.: Thermophysical property anomalies of
1266 Baltic seawater, Ocean Sci. 6, 949–981, https://doi.org/10.5194/os-6-949-2010, 2010b.

1267 Feistel, R., McDougall, T.J., and Millero. F.J.: Eine neue Zustandsgleichung für Meerwasser. DGM-
1268 Mitteilungen 2/2006, 19-21, 2006.

1269 Feistel, R., Tailleux, R., and McDougall, T. (eds.): Thermophysical Properties of Seawater, Copernicus,
1270 Göttingen, Germany, https://os.copernicus.org/articles/special_issue14.html, 2008a.

1271 Feistel, R. and Wagner, W.: High-pressure thermodynamic Gibbs functions of ice and sea ice, J. Mar.
1272 Res. 63, 95–139, https://elischolar.library.yale.edu/journal_of_marine_research/73 , 2005. [former
1273 DOI: 10.1357/0022240053693789 is invalid now]

1274 Feistel, R. and Wagner, W.: A new equation of state for H2O ice Ih, J. Phys. Chem. Ref. Data 35, 1021–
1275 1047, https://doi.org/10.1063/1.2183324, 2006.

1276 Feistel, R. and Wagner, W.: Sublimation pressure and sublimation enthalpy of H_2O ice Ih between 0
1277 and 273.16 K, Geochim. Cosmochim. Acta 71, 36–45, https://doi.org/10.1016/j.gca.2006.08.034,
1278 2007.

1279 Feistel, R., Wagner, W., Tchijov, V., and Guder, C.: Numerical implementation and oceanographic
1280 application of the Gibbs potential of ice, Ocean Sci., 1, 29–38, https://doi.org/10.5194/os-1-29-2005,
1281 2005.

1282 Feistel, R., Weinreben, S., Wolf, H., Seitz, S., Spitzer, P., Adel, B., Nausch, G., Schneider, B., and
1283 Wright, D.G.: Density and Absolute Salinity of the Baltic Sea 2006–2009, Ocean Sci. 6, 3–24,
1284 https://doi.org/10.5194/os-6-3-2010, 2010c.

1285 Feistel, R., Wielgosz, R., Bell, S.A., Camões, M.F., Cooper, J.R., Dexter, P., Dickson, A.G., Fisicaro, P.,
1286 Harvey, A.H., Heinonen, M., Hellmuth, O., Kretzschmar, H.-J., Lovell-Smith, J.W., McDougall, T.J.,
1287 Pawlowicz, R., Ridout, R., Seitz, S., Spitzer, P., Stoica, D., and Wolf, H.: Metrological challenges for
1288 measurements of key climatological observables: Oceanic salinity and pH, and atmospheric humidity.
1289 Part 1: overview, Metrologia 53, R1–R11, https://doi.org/10.1088/0026-1394/53/1/R1, 2016a.

1290 Feistel, R., Wright, D.G., Jackett, D.R., Miyagawa, K., Reissmann, J.H., Wagner, W., Overhoff, U.,
1291 Guder, C., Feistel, A., and Marion, G.M.: Numerical implementation and oceanographic application of
1292 the thermodynamic potentials of liquid water, water vapour, ice, seawater and humid air – Part 1:
1293 Background and equations, Ocean Sci. 6, 633–677, https://doi.org/10.5194/os-6-633-2010, 2010d.

1294 Feistel, R., Wright, D.G., Kretzschmar, H.-J., Hagen, E., Herrmann, S., and Span, R.: Thermodynamic
1295 properties of sea air, Ocean Sci. 6, 91–141, https://doi.org/10.5194/os-6-91-2010, 2010a.

1296 Feistel, R., Wright, D.G., Miyagawa, K., Harvey, A.H., Hruby, J., Jackett, D.R., McDougall, T.J., and
1297 Wagner, W.: Mutually consistent thermodynamic potentials for fluid water, ice and seawater: a new
1298 standard for oceanography, Ocean Sci. 4, 275–291, https://doi.org/10.5194/os-4-275-2008, 2008b.

1299 Flohn, H., Kapala, A., Knoche, H.R., and Mächel, H.: Water vapour as an amplifier of the greenhouse
1300 effect: new aspects, Meteorol. Zeitschrift, N.F. 1, 120-138,
1301 https://doi.org/10.1127/metz/1/1992/122, 1992.

1302 Fofonoff, N.P.: Interpretation of Oceanographic Measurements: Thermodynamics, Pacific
1303 Oceanographic Group, Nanaimo, B.C., 1958.

1304 Fofonoff, N.P.: Physical properties of sea-water, in: Hill, M.N. (ed.), The Sea, Wiley, New York, pp. 3-
1305 30, 1962.

1306 Fofonoff, N.P. and Millard Jr., R.C.: Algorithms for computation of fundamental properties of
1307 seawater, Unesco technical papers in marine science 44, Unesco, Paris,
1308 https://darchive.mblwhoilibrary.org/server/api/core/bitstreams/f77d18e9-e756-58eb-b042-
1309 a8870de55e3b/content, 1983.

1310 Foken, T.: 50 Jahre Monin-Obukhov'sche Ähnlichkeitstheorie, Universität Bayreuth, Abt.
1311 Mikrometeorologie, Bayreuth, Germany,
1312 https://www.baaycer.unibayreuth.de/mm/de/pub/html/2569605_Fo.pdf, 2004.

1313 Foken, T.: Angewandte Meteorologie, 3rd ed., Springer, Berlin, Germany, 2016.

1314 Foken, T., Hellmuth, O., Huwe, B., and Sonntag, D.: Physical Quantities, in: Foken, T. (ed.): Springer
1315 Handbook of Atmospheric Measurements, Springer Handbooks, Springer, Cham, pp. 107–151,
1316 https://doi.org/10.1007/978-3-030-52171-4_5, 2021.

1317 Foken, T. and Richter, S.H.: Konzept der Parametrisierung des Austauschs von Energie und
1318 Beimengungen in der bodennahen Luftschicht, Abh. Meteor. Dienst. DDR 146, 7–13, 1991.

1319 Foster, M.J., Phillips, C., Heidinger, A.K., Borbas, E.E., Li, Y., Menzel, P., Walther, A., and Weisz, E.:
1320 PATMOS-x Version 6.0: 40 Years of Merged AVHRR and HIRS Global Cloud Data, J. Climate 36, 1143-
1321 1160, https://doi.org/10.1175/JCLI-D-22-0147.1, 2023.

1322 Francis, J.A.: Vapor Storms, Scientific American Magazine 325, 26,
1323 https://doi.org/10.1038/scientificamerican1121-26, 2021.

1324 Gettelman, A. and Sherwood, S.C.: Processes Responsible for Cloud Feedback, Curr. Clim. Change
1325 Rep. 2, 179–189, https://doi.org/10.1007/s40641-016-0052-8, 2016.

1326 Gibbs, J.W.: Graphical methods in the thermodynamics of fluids, Transactions of the Connecticut
1327 Academy of Arts and Science 2, 309–342,
1328 https://www3.nd.edu/~powers/ame.20231/gibbs1873a.pdf, 1873a.

1329 Gibbs, J.W.: A Method of Graphical Representation of the Thermodynamic Properties of Substances
1330 by Means of Surfaces, Trans. Conn. Acad. Arts Sci. 2, 382–404,
1331 https://www3.nd.edu/~powers/ame.20231/gibbs1873b.pdf, 1873b.

1332 Gibbs, J.W.: On the equilibrium of heterogeneous substances, The Transactions of the Connecticut
1333 Academy of Arts and Science 3, 108–248, https://www.biodiversitylibrary.org/page/27725812, 1874-
1334 78.

1335 Gill, A.E.: Atmosphere-Ocean Dynamics, Academic Press, San Diego, 1982.

Gimeno, L., Nieto, R., Drumond, A., and Durán-Quesada, A.M.: Ocean Evaporation and Precipitation, in: Orcutt, J. (ed.): Earth System Monitoring: Selected Entries from the Encyclopedia of Sustainability Science and Technology, Springer, New York, NY, USA, https://doi.org/10.1007/978-1-4614-5684-1_13, 2013.

Glansdorff, P. and Prigogine, I.: Thermodynamic Theory of Structure, Stability and Fluctuations, Wiley-Interscience, London, 1971.

Graham, F.S., and McDougall, T.J.: Quantifying the Nonconservative Production of Conservative Temperature, Potential Temperature, and Entropy, J. Phys. Oceanogr. 43, 838–862, https://doi.org/10.1175/JPO-D-11-0188.1, 2013.

Guggenheim, E.A.: Thermodynamics, North-Holland, Amsterdam, 1949.

Gutzow, I.S. and Schmelzer, J.W.P.: Glasses and the Third Law of Thermodynamics, Chapter 9 in Schmelzer, J.W.P. and Gutzow, I.S. (eds), Glasses and the Glass Transition, Wiley-VCH, Weinheim, Germany, pp. 357–378, 2011.

Harvey, A.: Thermodynamic Properties of Water: Tabulation From the IAPWS Formulation 1995 for the Thermodynamic Properties of Ordinary Water Substance for General and Scientific Use, NIST Interagency/Internal Report (NISTIR), National Institute of Standards and Technology, Gaithersburg, MD, https://doi.org/10.6028/NIST.IR.5078, 1998.

Harvey, A.H., Hrubý, J., and Meier, K.: Improved and Always Improving: Reference Formulations for Thermophysical Properties of Water, J. Phys. Chem. Ref. Data 52, 011501, https://doi.org/10.1063/5.0125524, 2023.

Held, I.M. and Soden, B.J.: Robust Responses of the Hydrological Cycle to Global Warming, J. Climate 19, 5686-5699, https://doi.org/10.1175/JCLI3990.1, 2006.

Hellmuth, O. and Feistel, R.: Analytical Determination of the Nucleation-Prone, Low-Density Fraction of Subcooled Water, Entropy 22, 933, https://doi.org/10.3390/e22090933, 2020.

Hellmuth, O., Feistel, R., and Foken, T.: Intercomparison of different state-of-the-art formulations of the mass density of humid air, Bull. Atmos. Sci. & Technol. 2, 13, https://doi.org/10.1007/s42865-021-00036-7, 2021.

Hellmuth, O., Schmelzer, J.W.P., and Feistel, R.: Ice-Crystal Nucleation in Water: Thermodynamic Driving Force and Surface Tension. Part I: Theoretical Foundation, Entropy 22, 50, https://doi.org/10.3390/e22010050 , 2020.

Hellmuth, O. and Shchekin, A.K.: Determination of interfacial parameters of a soluble particle in a nonideal solution from measured deliquescence and efflorescence humidities, Atmos. Chem. Phys. 15, 3851–3871, https://doi.org/10.5194/acp-15-3851-2015, 2015.

Hirota, N., Ogura, T., Shiogama, H., Caldwell, P., Watanabe, M., Kamae, Y., and Suzuki, K.: Underestimated marine stratocumulus cloud feedback associated with overly active deep convection in models, Environ. Res. Lett. 16, 074015, https://doi.org/10.1088/1748-9326/abfb9e, 2021.

Holliday, N.P., Hughes, S.L., Borenäs, K., Feistel, R., Gaillard, F. Lavìn, A., Loeng, H., Mork, K.-A., Nolan, G., Quante, M. and Somavilla, R.: Chapter 3. Long-term Physical Variability in the North Atlantic Ocean, in: Reid, P.C. and Valdes, L. (eds.): ICES status report on climate change in the North Atlantic, ICES Cooperative Research Report 310, ICES, Copenhagen, p. 21-46, https://publications.hereon.de/id/29289/, 2011.

Holzapfel, W.B. and Klotz, S.: Coherent thermodynamic model for ice Ih - A model case for complex behaviour, J. Chem. Phys. 155, 024506, https://doi.org/10.1063/5.0049215, 2021.

Holzapfel, W.B. and Klotz, S.: Thermophysical properties of H_2O and D_2O ice Ih with contributions from proton disorder, quenching, relaxation, and extended defects: A model case for solids with quenching and relaxation, J. Chem. Phys. 160, 154508, https://doi.org/10.1063/5.0203614, 2024.

IAPWS AN6-16: Advisory Note No. 6: Relationship between Various IAPWS Documents and the International Thermodynamic Equation of Seawater—2010 (TEOS-10), The International Association for the Properties of Water and Steam, Dresden, Germany, http://www.iapws.org, 2016.

IAPWS G8-10: Guideline on an Equation of State for Humid Air in Contact with Seawater and Ice, Consistent with the IAPWS Formulation 2008 for the Thermodynamic Properties of Seawater (Niagara Falls, Canada: The International Association for the Properties of Water and Steam), available at: http://www.iapws.org, 2010.

IAPWS R10-06: Revised Release on the Equation of State 2006 for H2O Ice Ih (Doorwerth, The Netherlands: The International Association for the Properties of Water and Steam), available at: http://www.iapws.org, 2009.

IAPWS R13-08: Release on the IAPWS Formulation 2008 for the Thermodynamic Properties of Seawater, Berlin, Germany: The International Association for the Properties of Water and Steam, available at: http://www.iapws.org, 2008.

IAPWS R6-95: Revised Release on the IAPWS Formulation 1995 for the Thermodynamic Properties of Ordinary Water Substance for General and Scientific Use (Dresden, Germany: The International Association for the Properties of Water and Steam), available at: http://www.iapws.org, 2016.

IAPWS SR1-86: Revised Supplementary Release on Saturation Properties of Ordinary Water Substance, The International Association for the Properties of Water and Steam, St. Petersburg, Russia, http://www.iapws.org, 1992.

IOC, SCOR, and IAPSO: The international thermodynamic equation of seawater – 2010: Calculation and use of thermodynamic properties, Intergovernmental Oceanographic Commission, Manuals and Guides No. 56, UNESCO (English), 196 pp., Paris, https://unesdoc.unesco.org/ark:/48223/pf0000188170, 2010.

IOC-UNESCO: Resolution XXV-7 International Thermodynamic Equation of Seawater (TEOS-10), in: Proceedings of the Intergovernmental Oceanographic Commission, Twenty-Fifth Session of the Assembly, Paris, France, 16–25 June 2009, http://unesdoc.unesco.org/images/0018/001878/187890e.pdf, 2009.

IUGG: Resolution 4: Adoption of the International Thermodynamic Equation of Seawater–2010 (TEOS-10), In Proceedings of the International Union of Geodesy and Geophysics, XXV General Assembly, Melbourne, Australia, 27 June–7 July 2011, https://iugg.org/wp-content/uploads/2022/03/IUGG-Resolutions-XXV-GA-Melbourne-English.pdf, 2011.

Jackett, D.R., McDougall, T.J., Feistel, R., Wright, D.G., and Griffies, S.M.: Algorithms for Density, Potential Temperature, Conservative Temperature, and the Freezing Temperature of Seawater, Journal of Atmospheric and Oceanic Technology 23, 1709–1728, https://doi.org/10.1175/JTECH1946.1, 2006.

Ji, F., Pawlowicz, R., and Xiong, X.: Estimating the Absolute Salinity of Chinese offshore waters using nutrients and inorganic carbon data, Ocean Sci. 17, 909–918, https://doi.org/10.5194/os-17-909-2021, 2021.

Ji, F., Yang, J., Ding, F., Zheng, B., and Ning, P.: The salinity anomalies due to nutrients and inorganic carbon in the Bohai Sea, Front. Mar. Sci. 11, 1418860, https://doi.org/10.3389/fmars.2024.1418860, 2024.

Josey, S.A., Gulev, S., and Yu, L.: Exchanges through the ocean surface, in: Siedler, G., Griffies, S.M., Gould, J., and Church, J.A. (eds.): Ocean Circulation and Climate. A 21st Century Perspective, Elsevier, Amsterdam, The Netherlands, pp. 115–140, https://doi.org/10.1016/B978-0-12-391851-2.00005-2, 2013.

Josey, S.A., Kent, E.C., and Taylor, P.K.: New Insights into the Ocean Heat Budget Closure Problem from Analysis of the SOC Air–Sea Flux Climatology, J. Climate 12, 2856-2880, https://doi.org/10.1175/1520-0442(1999)012<2856:NIITOH>2.0.CO;2, 1999.

Kalisch, J. and Macke, A.: Radiative budget and cloud radiative effect over the Atlantic from ship-based observations, Atmos. Meas. Tech. 5, 2391–2401, https://doi.org/10.5194/amt-5-2391-2012, 2012.

Kittel, C.: Thermal Physics, Wiley, New York, 1969.

Köhler, H.: The nucleus in and the growth of hygroscopic droplets, Trans. Faraday Soc. 32, 1152–1161, https://doi.org/10.1039/tf9363201152, 1936.

Kozliak, E. and Lambert, F.L.: Residual Entropy, the Third Law and Latent Heat, Entropy 10, 274-284, https://doi.org/10.3390/e10030274, 2008.

Kraus, E.B. and Businger, J.A.: Atmosphere–Ocean Interaction, Oxford University Press/Clarendon, New York, Oxford, 1994.

Kretzschmar, H. J., Feistel, R., Wagner, W., Miyagawa, K., Harvey, A. H., Cooper, J. R., Hiegemann, M., Blangettit, F.L., Orlov, K.A., Weber, I., Singh, A., and Herrmann, S.: The IAPWS industrial formulation for the thermodynamic properties of seawater, Desalination and Water Treatment 55, 1177–1199, https://doi.org/10.1080/19443994.2014.925838, 2015.

Kuhlbrodt, T., Swaminathan, R., Ceppi, P., and Wilder, T.: A Glimpse into the Future: The 2023 Ocean Temperature and Sea Ice Extremes in the Context of Longer-Term Climate Change, Bulletin of the American Meteorological Society 105, E474–E485, https://doi.org/10.1175/BAMS-D-23-0209.1, 2024.

Lago, S., Giuliano Albo, P.A., von Rohden, C., and Rudtsch, S.: Speed of sound measurements in North Atlantic Seawater and IAPSO Standard Seawater up to 70 MPa, Marine Chemistry 177, 662-667, https://doi.org/10.1016/j.marchem.2015.10.007, 2015.

Laliberte, F.: Python bindings for TEOS-10, https://github.com/laliberte/pyteos_air, 2015.

Landau, L.D. and Lifschitz, E.M.: Statistische Physik, Akademie-Verlag, Berlin, 1966.

Landau, L.D. and Lifschitz, E.M.: Hydrodynamik, Akademie-Verlag, Berlin, 1974.

Le Menn, M., Giuliano Albo, P.A., Lago, S., Romeo, R., and Sparasci, F.: The absolute salinity of seawater and its measurands, Metrologia 56, 015005, https://doi.org/10.1088/1681-7575/aaea92 , 2018.

1457 Lemmon, E.W., Jacobsen, R.T, Penoncello, S.G., and Friend, D.G.: Thermodynamic Properties of Air
1458 and Mixtures of Nitrogen, Argon, and Oxygen From 60 to 2000 K at Pressures to 2000 MPa, J. Phys.
1459 Chem. Ref. Data 29, 331, https://doi.org/10.1063/1.1285884, 2000.

1460 Linke, F. and Baur, F.: Meteorologisches Taschenbuch, Geest & Portig, Leipzig, 1972.

1461 Liu, W. T., Katsaros, K.B., and Businger, J.A.: Bulk parameterizaJon of air-sea exchanges of heat and
1462 water vapor including the molecular constraints at the interface, J. Atmos. Sci. 36, 1722–1735,
1463 https://doi.org/10.1175/1520-0469(1979)036<1722:BPOASE>2.0.CO;2, 1979.

1464 Lovell-Smith, J.W., Feistel, R., Harvey, A.H., Hellmuth, O., Bell, S.A., Heinonen, M., and Cooper, J.R.:
1465 Metrological challenges for measurements of key climatological observables. Part 4: Atmospheric
1466 relative humidity, Metrologia 53, R39–R59, https://doi.org/10.1088/0026-1394/53/1/R40, 2016.

1467 Luo, H., Quaas, J., and Han, Y.: Diurnally asymmetric cloud cover trends amplify greenhouse warming,
1468 Science Advances 10, eado5179, https://doi.org/10.1126/sciadv.ado517, 2024.

1469 Manaure, E., Olivera-Fuentes, C., Wilczek-Vera, G., and Vera, J.H.: Pitzer Equations and a Model-Free
1470 Version of the Ion Interaction Approach for the Activity of Individual Ions, Chemical Engineering
1471 Science 241, 116619, https://doi.org/10.1016/j.ces.2021.116619, 2021.

1472 Margenau, H. and Murphy, G.M.: Die Mathematik für Physik und Chemie, B.G. Teubner, Leipzig,
1473 1964.

1474 Marion, G.M., Millero, F.J., and Feistel, R.: Precipitation of solid phase calcium carbonates and their
1475 effect on application of seawater S_A–T–P models, Ocean Sci. 5, 285–291, https://doi.org/10.5194/os-
1476 5-285-2009, 2009.

1477 Marion, G.M., Millero, F.J., Camões, F., Spitzer, P., Feistel, R., and Chen, C.-T.A.: pH of Seawater, Mar.
1478 Chem., 126, 89–96, https://doi.org/10.1016/j.marchem.2011.04.002, 2011.

1479 Marion, G.M., Mironenko, M.V., and Roberts, M.W.: FREZCHEM: A geochemical model for cold
1480 aqueous solutions, Computers & Geosciences 36, 10-15,
1481 https://doi.org/10.1016/j.cageo.2009.06.004, 2010.

1482 Martins, C.G. and Cross, J.: Technical note: TEOS-10 Excel – implementation of the Thermodynamic
1483 Equation Of Seawater – 2010 in Excel, Ocean Sci. 18, 627–638, https://doi.org/10.5194/os-18-627-
1484 2022, 2022.

1485 Maxwell, J.C.: Theory of Heat, Longmans, Green and Co., London and New York, 1888.

1486 McDougall, T.J.: Potential enthalpy: A conservative oceanic variable for evaluating heat content and
1487 heat fluxes, J. Phys. Oceanogr. 33, 945–963, https://doi.org/10.1175/1520-
1488 0485(2003)033<0945:PEACOV>2.0.CO;2, 2003.

1489 McDougall, T.J., Feistel, R., and Pawlowicz, R.: Chapter 6 - Thermodynamics of Seawater, in: Siedler,
1490 G., Griffies, S.M., Gould, J., and Church, J.A. (eds.): Ocean Circulation and Climate - A 21st Century
1491 Perspective, Academic Press, Oxford, pp. 141-158, https://doi.org/10.1016/B978-0-12-391851-
1492 2.00006-4, 2013.

1493 McDougall, T.J., Jackett, D.R., Millero, F.J., Pawlowicz, R., and Barker, P.M.: A global algorithm for
1494 estimating Absolute Salinity, Ocean Sci. 8, 1123–1134, https://doi.org/10.5194/os-8-1123-2012,
1495 2012.

1496 McDougall, T.J., Barker, P.M., Holmes, R.M., Pawlowicz, R., Griffies, S.M., and Durack, P.J.: The
1497 interpretation of temperature and salinity variables in numerical ocean model output and the

1498   calculation of heat fluxes and heat content, Geoscientific Model Development 14, 6445–6466,
1499   https://doi.org/10.5194/gmd-14-6445-2021, 2021.

1500   McDougall, T.J., Barker, P.M., Feistel, R., and Galton-Fenzi, B.K.: Melting of Ice and Sea Ice into
1501   Seawater and Frazil Ice Formation, Journal of Physical Oceanography 44, 1751–1775,
1502   https://doi.org/10.1175/JPO-D-13-0253.1, 2014.

1503   McDougall, T.J., Barker, P.M., Feistel, R., and Roquet, F.: A thermodynamic potential of seawater in
1504   terms of Absolute Salinity, Conservative Temperature, and in situ pressure, Ocean Sci. 19, 1719–
1505   1741, https://doi.org/10.5194/os-19-1719-2023 , 2023.

1506   MetOffice: New marine surface humidity climate monitoring product,
1507   https://www.metoffice.gov.uk/research/news/2020/new-marine-surface-humidity-climate-
1508   monitoring-product, 2020.

1509   Millero, F.J.: The thermodynamics of seawater. Part I. The PVT properties, Ocean Phys. Eng. 7, 403–
1510   460, https://www.researchgate.net/publication/289966693_THERMODYNAMICS_OF_SEAWATER_-
1511   _1_THE_PVT_PROPERTIES, 1982.

1512   Millero, F.J.: The Thermodynamics of Seawater. Part II. Thermochemical Properties, Ocean Phys. Eng.
1513   8, 1–40,
1514   https://www.researchgate.net/publication/289966823_THERMODYNAMICS_OF_SEAWATER_PART_II
1515   _THERMOCHEMICAL_PROPERTIES, 1983.

1516   Millero, F.J.: History of the Equation of State of Seawater, Oceanography 23, 18-33,
1517   https://doi.org/10.5670/oceanog.2010.21, 2010.

1518   Millero, F.J., Feistel, R., Wright, D.G., and McDougall, T.J.: The composition of Standard Seawater and
1519   the definition of the Reference-Composition Salinity Scale, Deep Sea Research Part I 55, 50-72,
1520   https://doi.org/10.1016/j.dsr.2007.10.001, 2008.

1521   Millero, F.J. and Huang, F.: The density of seawater as a function of salinity (5 to 70 g kg^{-1}) and
1522   temperature (273.15 to 363.15 K), Ocean Sci. 5, 91–100, https://doi.org/10.5194/os-5-91-2009,
1523   2009.

1524   Millero, F. J. and Huang, F.: Corrigendum to "The density of seawater as a function of salinity (5 to 70
1525   g kg^{-1}) and temperature (273.15 to 363.15 K)" published in Ocean Sci., 5, 91–100, 2009, Ocean Sci. 6,
1526   379–379, https://doi.org/10.5194/os-6-379-2010, 2010.

1527   Millero, F.J. and Leung, W.H.: The thermodynamics of seawater at one atmosphere, Am. J. Sci. 276,
1528   1035–1077, https://doi.org/10.2475/ajs.276.9.1035, 1976.

1529   Montgomery, R.B.: Observations of vertical humidity distribution above the ocean surface and their
1530   relation to evaporation, Pap. Phys. Oceanogr. Meteorol. 7, 2–30, https://doi.org/10.1575/1912/1099,
1531   1940.

1532   Morice, C.P., Kennedy, J.J., Rayner, N.A., and Jones, P.D.: Quantifying uncertainties in global and
1533   regional temperature change using an ensemble of observational estimates: The HadCRUT4 data set,
1534   J. Geophys. Res. 117, D08101, https://doi.org/10.1029/2011JD017187, 2012.

1535   Muhlbauer, A., McCoy, I.L., and Wood, R.: Climatology of stratocumulus cloud morphologies:
1536   microphysical properties and radiative effects, Atmos. Chem. Phys. 14, 6695–6716,
1537   https://doi.org/10.5194/acp-14-6695-2014, 2014.

Mulligan, J.F. and Hertz, G.G.: An unpublished lecture by Heinrich Hertz: "On the energy balance of the Earth", American Journal of Physics 65, 36-45, https://doi.org/10.1119/1.18565, 1997.

Myers, T.A., Scott, R.C., Zelinka, M.D., Klein, S.A., Norris, J.R., and Caldwell, P.: Observational Constraints on Low Cloud Feedback Reduce Uncertainty of Climate Sensitivity, Nature Climate Change 11, 501–507, https://doi.org/10.1038/s41558-021-01039-0, 2021.

Nayar, K.G., Sharqawy, M.H., Banchik, L.D., and Lienhard V, J.H.: Thermophysical properties of seawater: A review and new correlations that include pressure dependence, Desalination 390, 1-24, https://doi.org/10.1016/j.desal.2016.02.024, 2016.

Pawlowicz, R.: A model for predicting changes in the electrical conductivity, practical salinity, and absolute salinity of seawater due to variations in relative chemical composition, Ocean Sci. 6, 361–378, https://doi.org/10.5194/os-6-361-2010, 2010.

Pawlowicz, R.: Key Physical Variables in the Ocean: Temperature, Salinity, and Density. Nature Education Knowledge 4, 13, https://www.nature.com/scitable/knowledge/library/key-physical-variables-in-the-ocean-temperature-102805293/, 2013.

Pawlowicz, R.: Report to SCOR on JCS Activities Jun 2022 - Jun 2023, Joint SCOR/IAPWS/IAPSO Committee on the Properties of Seawater (JCS), https://scor-int.org/wp-content/uploads/2023/07/JCS-2023.pdf, 2023.

Pawlowicz, R. and Feistel, R.: Limnological applications of the Thermodynamic Equation of Seawater 2010 (TEOS-10), Limnology and Oceanography Methods 10, 853-867, https://doi.org/10.4319/lom.2012.10.853, 2012.

Pawlowicz, R., Feistel, R., McDougall, T.J., Ridout, P., Seitz, S., and Wolf, H.: Metrological challenges for measurements of key climatological observables. Part 2: Oceanic salinity, Metrologia 53, R12–R25, https://doi.org/10.1088/0026-1394/53/1/R12, 2016.

Pawlowicz, R., McDougall, T.J., Feistel, R., and Tailleux, R.: An historical perspective on the development of the Thermodynamic Equation of Seawater – 2010, Ocean Sci., 8, 161–174, https://doi.org/10.5194/os-8-161-2012 , 2012.

Pawlowicz, R., Wright, D.G., and Millero, F.J.: The effects of biogeochemical processes on oceanic conductivity/salinity/density relationships and the characterization of real seawater, Ocean Sci. 7, 363–387, https://doi.org/10.5194/os-7-363-2011, 2011.

Pawlowicz, R. and Yerubande, R.: Chapter 3 - Water as a Substance, in: Jones, I.D. and Smol, J.P. (eds): Wetzel's Limnology, Lake and River Ecosystems, Academic Press, p. 15-24, https://doi.org/10.1016/C2019-0-04412-3, 2024.

Peters-Lidard, C.D., Hossain, F., Leung, L.R., McDowell, N., Rodell, M., Tapiadore, F.J., Turk, F.J., and Wood, A.: 100 Years of Progress in Hydrology, American Meteorological Society, https://doi.org/10.1175/AMSMONOGRAPHS-D-18-0019.1, 2019.

Phillips, C. and Foster, M.J.: Cloudiness, in: Blunden, J., Boyer, T., and Bartow-Gillies, E. (eds.): State of the Climate in 2022, Bull. Amer. Meteor. Soc. 104, S60–S61, https://doi.org/10.1175/2023BAMSStateoftheClimate.1, 2023.

Pierrehumbert, R.T.: Principles of Planetary Climate, Cambridge University Press, Cambridge, 2010.

Pinker, R.T., Bentamy, A., Katsaros, K.B., Ma, Y., and Li, C.: Estimates of net heat fluxes over the Atlantic Ocean, J. Geophys. Res. Oceans 119, 1-18, https://doi.org/10.1002/2013JC009386, 2014.

1579   Planck, M.: Vorlesungen über die Theorie der Wärmestrahlung, Johann Ambrosius Barth, Leipzig,
1580   Germany, 1906.

1581   Pöhlker, M.L. et al.: Global organic and inorganic aerosol hygroscopicity and its effect on radiative
1582   forcing, Nature Communications 14, 6139, https://doi.org/10.1038/s41467-023-41695-8, 2023.

1583   Pollack, H.N., Hurter, S.J., and Johnson, J.R.: Heat Flow from the Earth's Interior: Analysis of the
1584   Global Data Set, Reviews of Geophysics 30, 267–280, https://doi.org/10.1029/93RG01249, 1993.

1585   Prigogine, I.: Etude Thermodynamique des Phénomènes Irreversibles (These, Bruxelles 1945),
1586   Desoer, Liege, Belgium, 1947.

1587   Prigogine, I. : Time, structure, and fluctuations (Nobel Lecture, 8 December 1977), Science 201, 777–
1588   785, https://doi.org/10.1126/science.201.4358.777, 1978.

1589   Randall, D.A.: Atmosphere, Clouds, and Climate, Princeton University Press, Princeton, 2012.

1590   Rapp, D.: Assessing Climate Change. Temperatures, Solar Radiation, and Heat Balance, Springer,
1591   Cham, Switzerland, 2014.

1592   Romer, R.H. (2001): Heat is not a noun. Amer. J. Phys. 69, 107–109,
1593   https://doi.org/10.1119/1.1341254

1594   Romps, D.M.: Exact Expression for the Lifting Condensation Level, Journal of the Atmospheric
1595   Sciences 74, 3891–3900, https://doi.org/10.1175/jas-d-17-0102.1, 2017.

1596   Roquet, F., Madec, G., McDougall, T.J., and Barker, P.M.: Accurate polynomial expressions for the
1597   density and specific volume of seawater using the TEOS-10 standard, Ocean Modelling 90, 29-43,
1598   https://doi.org/10.1016/j.ocemod.2015.04.002, 2015.

1599   Safarov, J., Berndt, S., Millero, F., Feistel, R., Heintz, A., and Hassel, E.: (p,ρ,T) properties of seawater:
1600   Extensions to high salinities, Deep Sea Research Part I 65, 146-156,
1601   https://doi.org/10.1016/j.dsr.2012.03.010, 2012.

1602   Safarov, J., Berndt, S., Millero, F.J., Feistel, R., Heintz, A., and Hassel, E.P.: (p,ρ,T) Properties of
1603   seawater at brackish salinities: Extensions to high temperatures and pressures, Deep Sea Research
1604   Part I 78, 95-101, https://doi.org/10.1016/j.dsr.2013.04.004, 2013.

1605   Safarov, J., Millero, F., Feistel, R., Heintz, A., and Hassel, E.: Thermodynamic properties of standard
1606   seawater: extensions to high temperatures and pressures, Ocean Sci. 5, 235–246,
1607   https://doi.org/10.5194/os-5-235-2009, 2009.

1608   Sharqawy, M.H., Lienhard V, J.H., and Subair, S.M.: Thermophysical properties of seawater: a review
1609   of existing correlations and data, Desalination and Water Treatment 16, 354-380,
1610   https://doi.org/10.5004/dwt.2010.1079, 2010.

1611   Schmelzer, J.W.P. and Tropin, T.V.: Glass Transition, Crystallization of Glass-Forming Melts, and
1612   Entropy, Entropy 20, 103, https://doi.org/10.3390/e20020103, 2018.

1613   Schmidt, G. (2024): Climate models can't explain 2023's huge heat anomaly - we could be in
1614   uncharted territory. Nature 627, 467. https://doi.org/10.1038/d41586-024-00816-z

1615   Schmidt, H., Seitz, S., Hassel, E., and Wolf, H.: The density–salinity relation of standard seawater,
1616   Ocean Sci. 14, 15–40, https://doi.org/10.5194/os-14-15-2018, 2018.

Schmidt, H., Wolf, H., and Hassel, E.: A method to measure the density of seawater accurately to the level of 10^{-6}, Metrologia 53, 770, https://doi.org/10.1088/0026-1394/53/2/770, 2016.

Seitz, S., Feistel, R., Wright, D.G., Weinreben, S., Spitzer, P., and De Bièvre, P.: Metrological traceability of oceanographic salinity measurement results, Ocean Sci. 7, 45–62, https://doi.org/10.5194/os-7-45-2011, 2011.

Seitz, S., Spitzer, P., and Brown, R.J.C.: CCQM-P111 study on traceable determination of practical salinity and mass fraction of major seawater components, Accred. Qual. Assur. 15, 9–17, https://doi.org/10.1007/s00769-009-0578-8, 2010.

Shirai, K.: Residual Entropy of Glasses and the Third Law Expression. Condensed Matter, preprint, https://doi.org/10.48550/arXiv.2207.11421, 2023.

Smythe-Wright, D., Gould, W. J., McDougall, T. J., Sparnocchia, S., and Woodworth, P. L.: IAPSO: tales from the ocean frontier, Hist. Geo Space. Sci., 10, 137–150, https://doi.org/10.5194/hgss-10-137-2019, 2019.

Sommerfeld, A.: Thermodynamik und Statistik, Verlag Harri Deutsch, Thun, 1988.

Spänkuch, D., Hellmuth, O., and Görsdorf, U.: What Is a Cloud? Bulletin of the American Meteorological Society 103, E1894-E1929, https://doi.org/10.1175/BAMS-D-21-0032.1, 2022.

Spall, M.A., Heywood, K., Kessler, W., Kunze, E., MacCready, P., Smith, J.A., Speer, K., and Fernau, M.E.: EDITORIAL, Journal of Physical Oceanography 43, 837, https://doi.org/10.1175/JPO-D-13-082.1, 2013.

Stewart, R.H.: Introduction to Physical Oceanography, Texas A & M University: College Station, TX, USA, https://doi.org/10.1119/1.18716, 2008.

Sun, H., Feistel, R., Koch, M., and Markoe, A.: New equations for density, entropy, heat capacity, and potential temperature of a saline thermal fluid, Deep Sea Research I 55, 1304-1310, https://doi.org/10.1016/j.dsr.2008.05.011

Sverdrup, H.U.: Das maritime Verdunstungsproblem, Annalen der Hydrographie und maritimen Meteorologie 64, 41-47, 1936.

Sverdrup, H.U.: On the Evaporation from the Oceans, J. Marine Research 1, 2-14, https://elischolar.library.yale.edu/journal_of_marine_research/515, 1937.

Tailleux, R.: Understanding mixing efficiency in the oceans: do the nonlinearities of the equation of state for seawater matter? Ocean Sci. 5, 271–283, https://doi.org/10.5194/os-5-271-2009, 2009.

Tailleux, R.: Entropy versus APE production: on the buoyancy power input in the oceans energy cycle, Geophys. Res. Lett. 37, L22602, https://doi.org/10.1029/2010GL044962, 2010.

Tailleux, R.: Local available energetics of multicomponent compressible stratified fluids, J. Fluid Mech. Rapids 842, 10 May 2018, R1, https://doi.org/10.1017/jfm.2018.196, 2018.

Tailleux, R. and Dubos, T.: A Simple and transparent method for improving the energetics and thermodynamics of seawater approximations: Static energy asymptotics (SEA), Ocean Modelling 188, 102339, https://doi.org/10.1016/j.ocemod.2024.102339, 2024.

Takada, A., Conradt, R., and Richet, P.: Residual entropy and structural disorder in glass: A review of history and an attempt to resolve two apparently conflicting views, Journal of Non-Crystalline Solids 429, 33-44, https://doi.org/10.1016/j.jnoncrysol.2015.08.019, 2015.

Thol, M., Pohl, S.M., Saric, D., Span, R., and Vrabec, J.: Fundamental equation of state for mixtures of nitrogen, oxygen, and argon based on molecular simulation data. J. Chem. Phys. 160, 174102, https://doi.org/10.1063/5.0188232, 2024.

Tchijov, V., Cruz-León, G., Rodríguez-Romo, S., and Feistel, R.: Thermodynamics of ice at high pressures and low temperatures, Journal of Physics and Chemistry of Solids 69, 1704-1710, https://doi.org/10.1016/j.jpcs.2007.12.018, 2008.

Turner, D.R., Achterberg, E.P., Chen, C.-T.A., Clegg, S.L., Hatje, V., Maldonado, M.T., Sander, S.G., van den Berg, C.M.G., and Wells, M.: Toward a Quality-Controlled and Accessible Pitzer Model for Seawater and Related Systems, Front. Mar. Sci. 3, https://doi.org/10.3389/fmars.2016.00139, 2016.

Uchida, H., Kawano, T., Nakano, T., Wakita, M., Tanaka, T., and Tanihara, S.: An Expanded Batch-to-Batch Correction for IAPSO Standard Seawater, Journal of Atmospheric and Oceanic Technology 37, 1507–1520, https://doi.org/10.1175/JTECH-D-19-0184.1, 2020.

Uchida, H., Kayukawa, Y., and Maeda, Y.: Ultra high-resolution seawater density sensor based on a refractive index measurement using the spectroscopic interference method, Sci. Rep. 9, 1548,. https://doi.org/10.1038/s41598-019-52020-z, 2019.

Ulfsbo, A., Abbas, Z., and Turner, D.R.: Activity coefficients of a simplified seawater electrolyte at varying salinity (5–40) and temperature (0 and 25 °C) using Monte Carlo simulations, Marine Chemistry 171, 78-86, https://doi.org/10.1016/j.marchem.2015.02.006, 2015.

Unesco: Background papers and supporting data on the International Equation of State of Sea water 1980, Unesco Technical Paper Marine Science 38, UNESCO, Paris, https://www.jodc.go.jp/info/ioc_doc/UNESCO_tech/047363eb.pdf, 1981.

Valladares, J., Fennel, W., and Morozov, E.G.: Announcement: Replacement of EOS-80 with the International Thermodynamic Equation of Seawater – 2010 (TEOS-10), Deep-Sea Res. 58, 978, https://doi.org/10.1016/j.dsr.2011.07.005. Ocean Modeling 40, 1, https://doi.org/10.1016/S1463-5003(11)00154-5, 2011.

Von Rohden, C., Fehres, F., and Rudtsch, S.: Capability of pure water calibrated time-of-flight sensors for the determination of speed of sound in seawater, J. Acoust. Soc. Am. 138, 651–662, https://doi.org/10.1121/1.4926380, 2015

Von Rohden, C., Weinreben, S., and Fehres, F.: The sound speed anomaly of Baltic seawater, Ocean Sci. 12, 275–283, https://doi.org/10.5194/os-12-275-2016, 2016.

Von Schuckmann, K., Minère, A., Gues, F., Cuesta-Valero, F.J., Kirchengast, G., Adusumilli, S., Straneo, F., Ablain, M., Allan, R.P., Barker, P., et al.: Heat stored in the Earth system 1960–2020: Where does the energy go? Earth Syst. Sci. Data 15, 1675–1709, https://doi.org/10.5194/essd-15-1675-2023, 2023.

Vose, R.S., Adler, R., Gu, G., Schneider, U., and Yin, X.: Precipitation, in: Blunden, J., Boyer, T., and Bartow-Gillies, E. (eds.): State of the Climate in 2022, Bull. Amer. Meteor. Soc. 104, S57, https://doi.org/10.1175/BAMS-D-23-0090.1, 2023.

Wagner, W. and Pruß, A.: The IAPWS Formulation 1995 for the Thermodynamic Properties of Ordinary Water Substance for General and Scientific Use, J. Phys. Chem. Ref. Data 31, 387–535, https://doi.org/10.1063/1.1461829, 2002.

1697 Wagner, W., Riethmann, T., Feistel, R., and Harvey, A.H.: New Equations for the Sublimation Pressure
1698 and Melting Pressure of H_2O Ice Ih, J. Phys. Chem. Ref. Data 40, 043103,
1699 https://doi.org/10.1063/1.3657937, 2011.

1700 Waldmann, C., Fischer, P.F., Seitz, S., Köllner, M., Fischer, J.-G., Bergenthal, M., Brix, H., Weinreben,
1701 S., and Huber, R.: A Methodology to Uncertainty Quantification of Essential Ocean Variables,
1702 Frontiers in Marine Science 9, 1002153, https://doi.org/10.3389/fmars.2022.1002153, 2022.

1703 Wang, H., Zheng, X.-T., Cai, W., and Zhou, L.: Atmosphere teleconnections from abatement of China
1704 aerosol emissions exacerbate Northeast Pacific warm blob events, PNAS 121, e2313797121,
1705 https://doi.org/10.1073/pnas.2313797121, 2024.

1706 Weinreben, S. and Feistel, R.: Anomalous salinity-density relations of seawater in the eastern central
1707 Atlantic, Deep–Sea Research I 154, 103160, https://doi.org/10.1016/j.dsr.2019.103160, 2019.

1708 Weller, R.A., Lukas, R., Potemra, J., Plueddemann, A.J., Fairall, C., and Bigorre, S.: Ocean Reference
1709 Stations: Long-Term, Open-Ocean Observations of Surface Meteorology and Air–Sea Fluxes Are
1710 Essential Benchmarks, Cover. Bull. Am. Meteorol. Soc. 103, E1968–E1990,
1711 https://doi.org/10.1175/BAMS-D-21-0084.1, 2022.

1712 Wikipedia: TEOS-10, https://en.wikipedia.org/wiki/TEOS-10, 2024.

1713 Willett, K.M., Simmons, A.J., Bosilovich, M., and Lavers, D.A.: Surface Humidity, in: Blunden, J., Boyer,
1714 T., and Bartow-Gillies, E. (eds.): State of the Climate in 2022, Bull. Amer. Meteor. Soc., 104 (9), S49-
1715 S52, https://doi.org/10.1175/2023BAMSStateoftheCli-1262 mate.1, 2023.

1716 WMO: Provisional State of the Global Climate 2023, World Meteorological Organization, Geneva,
1717 https://wmo.int/publication-series/provisional-state-of-global-climate-2023, 2024.

1718 Wood, R.: Stratocumulus Clouds, Monthly Weather Review 140, 2373-2423,
1719 https://doi.org/10.1175/MWR-D-11-00121.1, 2012.

1720 Woosley, R.J., Huang, F., and Millero, F.J.: Estimating absolute salinity (S_A) in the world's oceans using
1721 density and composition, Deep Sea Research Part I 93, 14-20,
1722 https://doi.org/10.1016/j.dsr.2014.07.009, 2014.

1723 Wright, D.G., Feistel, R., Reissmann, J.H., Miyagawa, K., Jackett, D.R., Wagner, W., Overhoff, U.,
1724 Guder, C., Feistel, A., and Marion, G.M.: Numerical implementation and oceanographic application of
1725 the thermodynamic potentials of liquid water, water vapour, ice, seawater and humid air – Part 2:
1726 The library routines, Ocean Sci. 6, 695–718, https://doi.org/10.5194/os-6-695-2010, 2010.

1727 Wright, D.G., Pawlowicz, R., McDougall, T.J., Feistel, R., and Marion, G.M.: Absolute Salinity, ''Density
1728 Salinity'' and the Reference-Composition Salinity Scale: present and future use in the seawater
1729 standard TEOS-10, Ocean Sci. 7, 1–26, https://doi.org/10.5194/os-7-1-2011, 2011.

1730 Wüst, G.: Die Verdunstung auf dem Meere, Veröffentlichungen des Instituts für Meereskunde an der
1731 Universität Berlin, Neue Folge, A. Geographisch-naturwissenschaftliche Reihe 6, 1–95, 1920.

1732 You, X.: Oceans break heat records five years in a row. The heat stored in the world's oceans
1733 increased by the greatest margin ever in 2023, Nature 625, 434-435,
1734 https://doi.org/10.1038/d41586-024-00081-0, 2024.

1735 Young, W.R.: Dynamic Enthalpy, Conservative Temperature, and the Seawater Boussinesq
1736 Approximation, Journal of Physical Oceanography 40, 394-400,
1737 https://doi.org/10.1175/2009JPO4294.1, 2010.

1738 Yu, L.: Global Variations in Oceanic Evaporation (1958–2005): The Role of the Changing Wind Speed,
1739 J. Climate 20, 5376-5390, https://doi.org/10.1175/2007JCLI1714.1, 2007.

1740 Zhang, W., Furtado, K., Wu, P., Zhou, T., Chadwick, R., Marzin, C., Rostron, J., and Sexton, D.:
1741 Increasing precipitation variability on daily-to-multiyear time scales in a warmer world, Science
1742 Advances 7, eabf8021, https://doi.org/10.1126/sciadv.abf8021, 2021.